MOLECULAR AND CELLULAR BIOLOGY, Nov. 2000, p. 8264–8282 Vol. 20, No. 21
0270-7306/00/$04.00+0

Elevated Levels of Hepatocyte Nuclear Factor 3β in Mouse Hepatocytes Influence Expression of Genes Involved in Bile Acid and Glucose Homeostasis

FRANCISCO M. RAUSA,[1] YONGJUN TAN,[1] HEPING ZHOU,[1] KYUNG W. YOO,[1] DONNA BEER STOLZ,[2] SIMON C. WATKINS,[2] ROBERTA R. FRANKS,[1] TERRY G. UNTERMAN,[1,3] AND ROBERT H. COSTA[1]*

Departments of Molecular Genetics, Medicine, Physiology, and Biophysics, College of Medicine, University of Illinois at Chicago,[1] and VA West Side Medical Center,[3] Chicago, Illinois 60607-7170, and Center for Biologic Imaging, University of Pittsburgh, Pittsburgh, Pennsylvania 15261[2]

Received 9 March 2000/Returned for modification 2 May 2000/Accepted 12 July 2000

The winged helix transcription factor, hepatocyte nuclear factor-3β (HNF-3β), mediates the hepatocyte-specific transcription of numerous genes important for liver function. However, the in vivo role of HNF-3β in regulating these genes remains unknown because homozygous null *HNF3*β mouse embryos die in utero prior to liver formation. In order to examine the regulatory function of HNF-3β, we created transgenic mice in which the −3-kb transthyretin promoter functions to increase hepatocyte expression of the rat HNF-3β protein. Postnatal transgenic mice exhibit growth retardation, depletion of hepatocyte glycogen storage, and elevated levels of bile acids in serum. The retarded growth phenotype is likely due to a 20-fold increase in hepatic expression of insulin-like growth factor binding protein 1 (IGFBP-1), which results in elevated levels in serum of IGFBP-1 and limits the biological availability of IGFs required for postnatal growth. The defects in glycogen storage and serum bile acids coincide with diminished postnatal expression of hepatocyte genes involved in gluconeogenesis (phosphoenolpyruvate carboxykinase and glycogen synthase) and sinusoidal bile acid uptake (Ntcp), respectively. These changes in gene transcription may result from the disruptive effect of HNF-3β on the hepatic expression of the endogenous mouse HNF-3α,-3β, -3γ, and -6 transcription factors. Furthermore, adult transgenic livers lack expression of the canalicular phospholipid transporter, mdr2, which is consistent with ultrastructure evidence of damage to transgenic hepatocytes and bile canaliculi. These transgenic studies represent the first in vivo demonstration that the HNF-3β transcriptional network regulates expression of hepatocyte-specific genes required for bile acid and glucose homeostasis, as well as postnatal growth.

The liver performs essential functions in the body by uniquely expressing both hepatocyte-specific genes encoding plasma proteins and enzymes involved in the detoxification and in the homeostasis of glucose, cholesterol, and bile salts (4). Functional analysis of numerous hepatocyte-specific promoter and enhancer regions reveals that they are composed of multiple *cis*-acting DNA sequences that bind different families of hepatocyte nuclear factors (HNF) (reviewed in reference 4). These include the HNF-1, HNF-3, HNF-4, CCAAT/enhancer binding protein (C/EBP), HNF-6, and fetoprotein transcription factor families (4, 29, 15, 52, 53, 57). Although none of these transcriptional regulatory proteins is entirely liver specific, the requirement for combinatorial protein interactions among them in order to achieve abundant transcriptional activity plays an important role in maintaining hepatocyte-specific gene expression.

The HNF-3 proteins are members of an extensive family of transcription factors that share homology in the winged helix DNA binding domain and use a modified helix-turn-helix motif to bind DNA as a monomer (8, 37). To date, the winged helix family consists of over 50 members, which play important roles in the differentiation of distinct cellular lineages in *C. elegans, Drosophila*, rodents, and humans (25). The rodent HNF-3α, -3β, and -3γ proteins were originally identified as factors mediating liver-specific transcription of the transthyretin (TTR) (10, 27, 28) gene, encoding a serum carrier protein of thyroxine and vitamin A, and were later shown to regulate the expression of other genes critical for liver function. Subsets of these hepatocyte genes include the serum carrier proteins albumin, α-fetoprotein, and apolipoprotein AI (21, 34, 39); the cholesterol 7α-hydroxylase (Cyp7A) enzyme involved in bile acid synthesis (9, 40, 71); and the glucose metabolism enzymes 6-phosphofructo-2-kinase/fructose-2,6-bisphosphatase (PFK-2) and glucose 6-phosphatase (G6P) (31, 33, 54). HNF-3 proteins also recognize the insulin response elements of phosphoenolpyruvate carboxykinase (PEPCK) and insulin-like growth factor binding protein 1 (IGFBP-1) genes (66, 72) and participate in growth hormone activation of insulin-like growth factor 1 (IGF-1) (43). A hepatoma cell line which expresses a dominant-negative HNF-3 mutant specifically extinguished transcription of HNF-3 target genes (68). In support of HNF-3's role in regulating the transcription of hepatocyte-specific genes during early mouse liver development, induction of albumin expression during hepatic specification coincides with in vivo footprinting of the HNF-3 binding sites in the albumin enhancer region (78). Moreover, in vivo footprinting and nucleosome assembly studies of the −10-kb albumin enhancer region have demonstrated that the HNF-3 proteins are involved in organizing the nucleosome architecture of the albumin enhancer sequences (7, 38, 60).

In the mouse embryo, HNF-3β expression initiates during gastrulation in the node, notochord mesoderm, and floorplate

* Corresponding author. Mailing address: Department of Molecular Genetics (M/C 669), University of Illinois at Chicago, College of Medicine, 900 S. Ashland Ave., Rm. 2220 MBRB, Chicago, IL 60607-7170. Phone: (312) 996-0474. Fax: (312) 355-4010. E-mail: RobCosta@uic.edu.

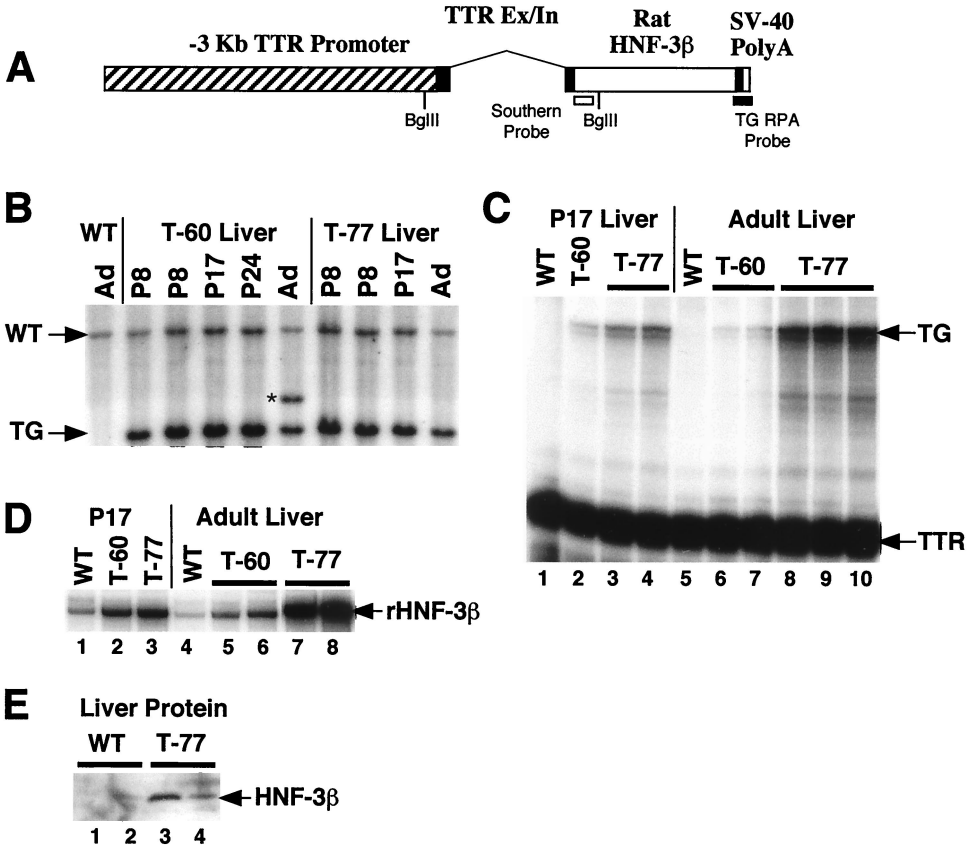

FIG. 1. The −3-kb TTR promoter directs hepatic HNF-3β transgene expression. (A) Representation of the mouse −3-kb TTR promoter–HNF-3β transgene construct. Transgenic mice were created with the −3-kb TTR promoter region (striped box) driving expression of the rat HNF-3β cDNA (open box), which was cloned into the TTR second exon (solid box) that contains the SV40 polyadenylation signal (10, 74, 76, 77). (B) Southern blot analysis of wild-type (WT) and transgenic liver DNA. Genomic DNA was prepared from P8, P17, P24, and adult transgenic (T-60 and T-77) and wild-type mouse livers, digested with *Bgl*II, and then analyzed by Southern blots using the 5′ *Bgl*II rat HNF-3β cDNA probe (see panel A). Indicated are the positions of hybridizing *Bgl*II bands from wild-type and transgenic (TG) loci and a band resulting from partial digestion (*). (C) Analysis of HNF-3β transgene expression in mouse liver. Total liver RNA was isolated from either P17 (lanes 1 to 4) or adult (lanes 5 to 10) liver and used for RNase protection assays with the TTR-SV40 transgene antisense-labeled RNA probe (see Materials and Methods). As reported previously, RNase protection of the HNF-3β transgene produces a 310-nucleotide product (TG), whereas RNase protection of the endogenous mouse TTR second exon yields a 90-nucleotide band (74, 76, 77). (D) Analysis of rat HNF-3β transgene expression in mouse liver. Total liver RNA from either P17 (lanes 1 to 3) or adult mouse (lanes 4 to 8) liver was used for RNase protection assays of the rat HNF-3β antisense-labeled RNA probes. Note that hepatic mRNA levels of the HNF-3β transgene in the T-60 transgenic line displays a 50% reduction from P17 to adult mice, whereas its expression displays a twofold increase in the T-77 line during the same time period. (E) Increased hepatic HNF-3β protein levels in the T-77 transgenic mouse line. HNF-3β protein expression was analyzed in liver protein extracts from either wild-type or T-77 transgenic (5-week-old) mice by Western blot analysis using an affinity-purified HNF-3β antibody (see Materials and Methods).

neuroepithelium and in visceral and definitive endoderm (2, 41, 56, 59). Consistent with this expression pattern, homozygous null *Hnf3*β embryos die in utero because of defective formation of the node, notochord, and visceral endoderm, which are required for development of the primitive streak during gastrulation and inductive signaling for neurotube formation (1, 73). Tetraploid rescue of the visceral endoderm defect in *Hnf3*$\beta^{-/-}$ embryos restored normal primitive streak morphogenesis, but the embryos failed to undergo proper gastrulation because they were still missing the node and notochord and did not develop foregut and midgut endoderm (12). This *Hnf3*$\beta^{-/-}$ embryo defect has thereby precluded examination of the in vivo function of HNF-3β in the regulation of its hepatocyte target genes.

To assess the role of HNF-3β in hepatocyte-specific gene regulation, we have increased hepatocyte HNF-3β levels in transgenic mice using the −3-kb TTR promoter region (74, 76, 77). Our studies show that postnatal transgenic mice exhibit growth retardation, diminished liver glycogen storage, and elevated levels of bile acids in serum. These defects are coincident with diminished postnatal expression of hepatocyte genes involved in glucose and bile acid homeostasis. Furthermore, the TTR–HNF-3β transgenic mice display increased hepatic expression of IGFBP-1, which limits the biological effects of IGFs necessary for postnatal growth. Elevated HNF-3β levels also caused diminished hepatic expression of the endogenous mouse HNF-3α, -3β, -3γ, and -6 transcription factors, which may contribute to the observed changes in hepatocyte-specific gene expression. Moreover, we can state with certainty that diminished transgenic levels of HNF-3 and HNF-6 were specific because we observed normal adult hepatic expression of the HNF-1α, HNF-4α, C/EBPα, and C/EBPβ transcription factors.

MATERIALS AND METHODS

Generation of TTR–HNF-3β transgenic mice. The TTR minigene construct (Fig. 1A) consists of the −3-kb TTR promoter region, the first and second TTR exons fused to the simian virus 40 (SV40) 3′-end and poly(A) sequences (74, 76, 77). The 1.6-kb rat HNF-3β cDNA was excised with *Eco*RI, blunt ended with Klenow fragment of DNA polymerase I, and ligated into a unique *Stu*I site located in the second exon of the pTTR-exv3 minigene vector (Fig. 1A). The 6.0-kb *Hin*dIII fragment containing the −3-kb TTR promoter driving the rat HNF-3β cDNA expression was purified and then used to generate transgenic CD-1 mice as described previously (77). Four of the 51 CD-1 mice that were born

carried the TTR–HNF-3β transgene as identified by PCR analysis of genomic DNA extracted from mouse tails using primers described previously (74, 76, 77). The genotypes of PCR-positive mice were verified by Southern blot analysis using *Bgl*II digestion of genomic DNA and hybridization with a 500-nucleotide probe generated from the 5′ end of the rat HNF-3β cDNA as depicted in Fig. 1B. Two individual founder TTR–HNF-3β transgenic mice (T-60 and T-77) were mated with CD-1 wild-type mice to generate F_1 transgenic mice, which were used for analysis of the liver phenotype. A third transgenic mouse died shortly after weaning and a fourth transgenic founder (T-74) was a female possessing a mosaic transgene integration, as evidenced by the fact that 1 of her 14 offspring was transgenic (this line was not further analyzed).

Immunohistochemical staining and PAS-glycogen staining of paraffin-embedded liver sections. Livers were dissected from wild-type or transgenic embryos, postnatal mice, or adult mice, fixed in 4% paraformaldehyde in phosphate-buffered saline (PBS) at 4°C overnight, dehydrated, and embedded in paraffin. A microtome was used to make serial 7-μm sections of liver, which were collected on Superfrost Plus slides (Fisher), dried on a 40°C slide warmer overnight, and processed for immunohistochemistry using the microwave-based antigen retrieval method as described previously (77, 79). The sections were blocked with 3% normal serum and incubated with primary antibody diluted in 1% normal serum in Tris-buffered saline (TBS) overnight at 4°C (HNF-3β monoclonal antibody [4C7] was obtained from the University of Iowa Developmental Studies Hybridoma Bank; 1:4 dilution). Sections were then washed in TBS three times and incubated with secondary antibody diluted in 1% normal serum in TBS for 1 h at room temperature. Primary antibodies were detected using secondary anti-mouse immunoglobulin G coupled with horseradish peroxidase staining using the appropriate substrates (Vector Labs). Paraffin-embedded liver sections from postnatal wild-type and transgenic (T60 and T77) mice were stained for glycogen using the periodic acid-Schiff (PAS) reaction as described by Frederiks et al. (14).

HNF-6 antibody, EMSA, and Western blot. For the generation of an HNF-6 specific antibody, HNF-6 N-terminal sequences (amino acids 1 to 289) were fused to the glutathione *S*-transferase (GST) protein. Recombinant HNF-6 protein was isolated from bacterial cultures, purified to homogeneity via glutathione affinity chromatography (44), and used to immunize rabbits (rabbit immunization with GST–HNF-6 antigen was performed by the Biological Research Laboratory at the University of Illinois at Chicago [UIC]). Electrophoretic mobility shift assay (EMSA) with liver nuclear extracts and a high-affinity HNF-6 DNA binding site (derived from the HNF-3β promoter) was used to assess the specificity of the HNF-6 antibody by altering or supershifting the migration of the HNF-6 protein–DNA complex (50, 57). The supershift assay involved a preincubation step of liver nuclear protein extracts with either preimmune or HNF-6 rabbit antiserum (0.5 or 1 μl) for 45 min at room temperature prior to the EMSA binding reaction with the HNF-6 DNA binding site as described previously (50, 52, 57). We also included a blocking control which involved the addition of the GST–HNF-6 fusion protein (antigen) during the preincubation step. Recombinant GST protein was used to remove GST-specific antibodies and GST–HNF-6 fusion protein was used to affinity purify the HNF-6 antibody following protocols described previously (77). For Western blot analysis using the HNF-6 antibody, total liver protein extract was isolated from either wild-type or T-77 transgenic mice (5 weeks old) using a polytron homogenizer following the protocol described by Tsutsui et al. (65). A portion (200 μg) of total liver protein was subjected to sodium dodecyl sulfate (SDS)-polyacrylamide gel electrophoresis (PAGE) and then analyzed by Western blotting with either affinity-purified HNF-6 or HNF-3β antiserum (50, 57) using the ECL Plus Western blot detection reagents as described by the manufacturer (Amersham Pharmacia Biotech).

Serum preparation and analysis. Mice were anesthetized with methoxyflurane (Metofane; Schering-Plough Animal Health Corp., Union, N.J.), and a syringe was used to draw blood from the beating mouse heart through the atrium. Serum was generated from the blood following coagulation at 37°C for 30 min and at 4°C overnight, and precipitate was removed by centrifugation. The determination of the levels in serum of all bile acids, IGF-1, glucagon, and insulin and the levels in serum of postnatal day 8 (P8), P17, and adult wild-type, T-60, and T-77 mice were determined by Ani Lytics, Inc., Gaithersburg, Md. The serum measurements for eight wild-type and eight adult T-77 mice were also determined by the Biological Research Laboratory at UIC.

Western IGF-1 ligand blotting and immunoprecipitation of serum IGF binding proteins. Serum (2 μl) from 5-week-old T-77 transgenic or wild-type mice was loaded for nonreducing SDS-PAGE onto a 4 to 20% gradient gel and then transferred to nitrocellulose for Western blot analysis with IGF-1 ligand. Membranes were blocked, probed with [^{125}I]IGF-I and IGFBPs were detected by autoradiography, as previously reported (67). To examine levels in serum of immunoreactive IGFBP-1, specific antibodies for rodent IGFBP-1 (67) were adsorbed onto Pansorbin beads prior to incubation with serum (10 μl) from T-77 and wild-type mice. Bound proteins were eluted by heating with 1× nonreducing Laemmli sample buffer for 10 min at 100°C and then loaded for SDS-PAGE and Western ligand blotting as described above.

Light and transmission electron microscopy. Mouse livers were perfusion fixed through the heart with 2.5% glutaraldehyde in PBS. The livers were removed and immersed in the same fixative for 2 additional days at 4°C. Several 1-mm^3 cubes were removed from the liver, washed three times in PBS, and then postfixed in aqueous 1% OsO_4–1% $K_3Fe(CN)_6$ for 1 h. Following three PBS washes, the pellet was dehydrated through a graded series of 30 to 100% ethanol–100% propylene oxide and then infiltrated in a 1:1 mixture of propylene oxide-Polybed 812 epoxy resin (Polysciences, Warrington, Pa.) for 1 h. After several changes of 100% resin over 24 h, the pellet was embedded in molds and cured at 37°C overnight, followed by additional hardening at 65°C for two more days. Ultrathin (60-nm) sections were collected on 200-mesh copper grids and stained with 2% uranyl acetate in 50% methanol for 10 min, followed by 1% lead citrate for 7 min. Sections were photographed using a JEOL JEM 1210 transmission electron microscope (JEOL, Peabody, Mass.) at 80 or 60 kV onto electron microscope-film (ESTAR thick base; Kodak, Rochester, N.Y.) and printed onto photographic paper. Thick sections (300 nm) were heated onto glass slides and stained with filtered 0.5% aqueous toluidine blue. Digital images of thick sections were acquired on a Nikon Microphot-FXL microscope equipped with a Sony 3CCD color video camera. Electron micrographs were digitized on a flatbed scanner at 400 pixels/in. (StudioStar; Agfa). Digitized images were assembled into montages using Adobe Photoshop 5.0.

RNA extraction and RNase One protection assay. Total RNA was extracted from mouse liver by an acid guanidium-thiocyanate-phenol-chloroform extraction method using RNA-STAT-60 (Tel-Test B, Inc., Friendswood, Tex.). RNase protection assay was performed with [α-^{32}P]UTP-labeled antisense RNA synthesized from plasmid templates with the appropriate RNA polymerase as previously described (10, 77). Quantitation of expression levels was done with scanned X-ray films using the BioMax 1D program (Kodak).

Synthesis of antisense TTR transgene, rat HNF-3β, and rat C/EBPβ probes was as described previously (50, 74, 76, 77). T7 RNA polymerase was used to synthesize the mouse HNF-3γ (accession no. X74938; bp 1354 to 1584), mouse HNF-3β (accession no. X74937; bp 1337 to 1668), and mouse HNF-3α (accession no. X74936; bp 1 to 150) probes using *Eco*RI-digested pBluescript (pBS) templates. SP6 RNA polymerase was used to synthesize the mouse HNF-6α probe (accession no. U95945; bp 1432 to 1603) using *Pvu*II-digested pGEM2 template. T7 RNA polymerase was used to synthesize the mouse HNF-1α probe (accession no. M57966; bp 383 to 769) using *Bam*HI-digested pCRII template. SP6 RNA polymerase was used to synthesize the rat C/EBPα probe (accession no. NM_012524) using *Pvu*II-digested pGEM-1 template. T3 RNA polymerase was used to synthesize the Rat HNF-4α probe (accession no. X57133; a gift from F. Sladek) using *Xho*I-digested pBS template. T3 RNA polymerase was used to synthesize the sister of rat P-glycoprotein (SPGP) probe (a gift from R. Green) using *Sty*I-digested pBS template. SP6 RNA polymerase was used to synthesize the rat cholesterol 7α-hydroxylase (Cyp7A) probe (a gift from J. Y. Chiang) using *Eco*RI-digested pGEM-1 template.

The following RNase protection probes were isolated by reverse transcription-PCR of adult mouse liver RNA (primer sequences are written in the 5′-to-3′ direction) and cloned into the pBS template, and antisense RNA probes were synthesized with either T7 RNA polymerase using *Not*I-digested template or T3 RNA polymerase using *Xho*I-digested template. T7 RNA polymerase was used to synthesize the canalicular multispecific organic anion transporter probe (cMoat: GACGGATAGCCTCATTCAGACG and AACTGTGTATCTGTGC CCCTATGAC), the organic anion-transporting polypeptide probe (Oatp: CGC ATAACTCCTCAGGATGCTC and TGGTAAGGATGCTTCTCAGAGACC), the Na^+-taurocholate cotransporting polypeptide probe (Ntcp; TGGAGTTCA GCAAGATCAAGGC and GGAGCAGGTGGTCATCACAATG), the glycogen phosphorylase probe (GP; CAATGTGGAGATGGCAGAGGAAG and ATGATGTCTTTGAAGAGGTCTGGC), the glycogen synthase probe (GS; GGGGAAGACAGTGAGCGTTATG and TCAAGAGTCTGGAGTGGGGT TCAG), and the G6P probe (G6P; TACCAAGGGAGGAAGGATGGAG and AAGACGAGGTTGAACCAGTCTCCG). T3 RNA polymerase was used to synthesize the glucokinase probe (GK; ACTTGAGGCAGCTATGTGCAGG and GCTGTCTCCAGAATCTGTGTACTG), the phosphoenolpyruvate carboxykinase probe (PEPCK; GCTGTGCCAGCCAGAGTATATTCAC and AATGATGACCGTCTTGCTTTCG), the PFK-2 probe (GTTGCGGTTTTTG ATGCCAC and TCCTCATCCAAAGGTTGGTAGTTG), and the IGFBP-1 probe (GATCGCCGACCTCAAGAAATG and ATGGGTAGACACACCAG CAGAGTC) using *Hin*dIII-digested pBS template and the IGFBP-3 probe (CC AACCTGCTCCAGGAAACATC and ACCGTATTCTGTCTCCCGCTTAG) and the IGF-1 probe (CGTCTTCACACCTCTTCTACCTGG and ATGTGGC ATTTTCTGCTCCGTGGG) using *Eco*NI-digested pBS template. Finally, SP-6 RNA polymerase was used to synthesize the multidrug resistance 2P-glycoprotein probe (mdr2; GCGGAATTCAGGCTGTGGTTTCCCCAGG and GCGG GATCCCCTGATGCTGCCTAGTTCAAA) using *Eco*RI-digested pGEM-1 template.

Methylation interference footprinting of the IGFBP-1 promoter sequence with recombinant HNF-3β protein. A double-stranded oligonucleotide containing −85 through −122 bp upstream from the transcription start site of the rat IGFBP-1 promoter was cloned into the *Mlu*I site of the pGL2 polylinker by blunt-end ligation (66). The polylinker was cut with *Hin*dIII, then treated with alkaline phosphatase, and finally cut again with *Sma*I and gel purified. The probe was labeled by end labeling with either T4 polynucleotide kinase in the presence of [γ-^{32}P]ATP or (exo-)Klenow in the presence of [α-^{32}P]dATP. The labeled probe was partially methylated with DMS (57); then 25 fmol was incubated with 500 ng of bacterially expressed GST–HNF-3β (44). Free and bound probes were separated by nondenaturing 6% PAGE and then excised, eluted, and purified with ELUTIPs as described by the manufacturer (Schleicher & Schuell). Probes

were ethanol precipitated in the presence of 25 μg of tRNA per ml and redissolved in sodium phosphate-EDTA buffer. The amounts of counts and tRNA in the free and bound probes were equalized. G and A residues were cleaved under alkaline conditions (probes were heated to 90°C for 15 min, cooled, and then heated again following the addition of NaOH). Cleavage products were precipitated with ethanol and sodium acetate and then redissolved and loaded for electrophoresis on an 8% polyacrylamide sequencing gel.

RESULTS

Hepatocyte expression of the HNF-3β transgene in T-60 and T-77 mouse lines. In order to examine the role of HNF-3β in liver function, we created transgenic CD-1 mice in which the −3-kb TTR promoter region was used to increase hepatocyte expression of the rat HNF-3β cDNA (74, 76, 77; Fig. 1A). Tail DNA from potential transgenic mice was screened for the presence of the TTR minigene by PCR analysis, and two transgenic CD-1 mouse lines (T-60 and T-77) were established for further characterization (data not shown). A 5′ HNF-3β cDNA probe was used to hybridize Southern blots containing size-fractionated *Bgl*II-digested genomic DNA prepared from either postnatal or adult transgenic mouse liver (Fig. 1A). Transgenic mouse genomic DNA from all stages of postnatal liver development possessed two hybridizing *Bgl*II bands: one corresponded to the endogenous mouse HNF-3β gene, and the other corresponded to an internal transgene fragment which is common to both mouse lines (Fig. 1B). To determine expression levels of the rat HNF-3β transgene during postnatal liver development, we performed RNase protection assays using total liver RNA with either the TTR transgene or the rat HNF-3β probes (see Materials and Methods). While the T-77 livers displayed a twofold increase in hepatic mRNA levels of the HNF-3β transgene from P17 to 6 weeks old, the T-60 line exhibited a 50% decline in hepatic transgene expression during the same postnatal period (Fig. 1C and D). To measure hepatic HNF-3β protein levels, liver protein extracts were prepared from either wild-type or T-77 transgenic mice (5 weeks old) and then used for Western blot analysis with affinity-purified polyclonal HNF-3β antibody (50). The Western blot demonstrates that the T-77 liver protein extracts displayed a fivefold increase in hepatic HNF-3β protein levels compared to wild-type liver extracts (Fig. 1E).

To further determine the HNF-3β protein levels in developing transgenic hepatocytes, an HNF-3β monoclonal antibody was used for immunohistochemical staining of paraffin-embedded liver sections prepared from either wild-type or transgenic (T-60 and T-77) mice. Embryonic day 17.5 (E17.5) and P8 transgenic mouse livers (T-60 and T-77) exhibited similar increases in levels of HNF-3β protein in hepatocytes (Fig. 2B, C, E, and F) compared to endogenous HNF-3β expression in wild-type livers (Fig. 2A and D). However, P17 livers from T-60 transgenic mice displayed a reduction in the number of hepatocytes expressing abundant levels of HNF-3β protein (Fig. 2H), which continues in older T-60 transgenic liver (Fig. 2K, arrows). By contrast, T-77 hepatocytes continued to abundantly express the HNF-3β transgene protein (Fig. 2I and L) compared to wild-type liver (Fig. 2G and J). Southern blot analysis of T-60 liver DNA from postnatal and adult transgenic mice showed that postnatal decline in transgene expression was not due to genomic rearrangement of the transgene (Fig. 1B). One possible explanation for the loss of T-60 transgene expression is that it has integrated into a chromosomal locus which is transcriptionally repressed in postnatal hepatocytes.

Postnatal reduction in TTR–HNF-3β transgenic mouse size correlates with increase in hepatic IGFBP-1 expression. We noted that, during the breeding process, both TTR–HNF-3β transgenic mouse lines weighed 50% less than their wild-type littermates by P10 and that this difference in body weight was more pronounced in the P30 mice of both transgenic lines (Fig. 3A and B). We were able to determine that this defect in postnatal growth is not due to hypoglycemia because comparable glucose levels were observed in the serum of postnatal transgenic and wild-type mice (Table 1). RNase protection assays were used to determine if there was an alteration in the hepatic expression of HNF-3β target genes that are required for postnatal growth. These include the growth hormone-regulated IGF-1A gene (3, 43, 49) and the gene encoding IGFBP-1, which limits the biological activity of serum IGFs (16, 51, 66). RNase protection assays demonstrated that postnatal T-60 and T-77 transgenic livers exhibited significant reductions in IGF-1A mRNA levels compared to wild-type livers (Fig. 3C). Consistent with reduced levels of the HNF-3β transgene protein in the adult T-60 liver, IGF-1A expression is normal, whereas in the adult T-77 line its hepatic mRNA levels remain diminished (Fig. 3D). Despite this reduction in the postnatal hepatic expression of IGF-1A, T-77 mice exhibited normal IGF-1 levels in serum compared to their P17 wild-type littermates (Table 1). This result suggests that the dramatic reduction in transgenic mouse size is unlikely due to diminished hepatic expression of IGF-1A. In P17 transgenic livers, we found an approximately 20-fold increase in the hepatic expression of IGFBP-1 (Fig. 3C), and this increase became less pronounced in adult transgenic mice (Fig. 3D). In contrast, the transgenic mice exhibited normal hepatic mRNA levels of another IGF carrier protein, IGFBP-3 (data not shown). Western blotting of serum followed by ligand binding with radioactively labeled IGF-1 protein reveals that the levels of 32-kDa IGF binding proteins are increased in serum from 5-week-old T-77 transgenic compared to wild-type mice, while the levels of 45- to 50-kDa and 24-kDa IGFBPs (corresponding to IGFBP-3 and -4, respectively) are similar in transgenic and wild-type mice (Fig. 3E, Neat panel). To determine whether this increase in 32-kDa IGFBPs reflects a change in the circulating levels of IGFBP-1, the IGFBP-1 protein was immune precipitated from either T-77 or wild-type mouse serum and then Western blots were analyzed for IGF-1 ligand binding (see Materials and Methods). Immunoreactive IGFBP-1 is readily detected in serum from T-77 transgenic but not wild-type mice, demonstrating that circulating levels of IGFBP-1 are markedly increased in the T-77 transgenic mouse line. The retarded growth of the TTR–HNF-3β transgenic mice is thus consistent with transgenic mouse studies demonstrating that increased hepatic expression of IGFBP-1 causes significant reductions in postnatal growth (16, 51). Methylation interference footprinting of the IGFBP-1 insulin response element (IRE) with recombinant HNF-3β protein demonstrates that this promoter sequence specifically binds the HNF-3β protein (Fig. 3F). Previous cotransfection studies demonstrated that HNF-3β protein is capable of stimulating IGFBP-1 promoter activity and that this transcriptional activation required retention of the HNF-3 binding sequence (66). Taken together, these studies are consistent with documentation regarding the ability of HNF-3β to stimulate transcription of the IGFBP-1 gene in vivo.

T-77 line exhibits diminished hepatocyte expression of the endogenous mouse HNF-3 isoforms and HNF-6. We next examined the possibility that observed changes in T-77 liver gene expression were mediated by altered expression of other liver transcription factors. To avoid cross-hybridization with the rat HNF-3β transgene, we used antisense RNA probes made to the divergent untranslated portion of the mouse HNF-3α, HNF-3β, and HNF-3γ genes for RNase protection assays (Fig. 4). To our surprise, P8 livers from both transgenic lines exhibited diminished expression of the endogenous mouse HNF-3α,

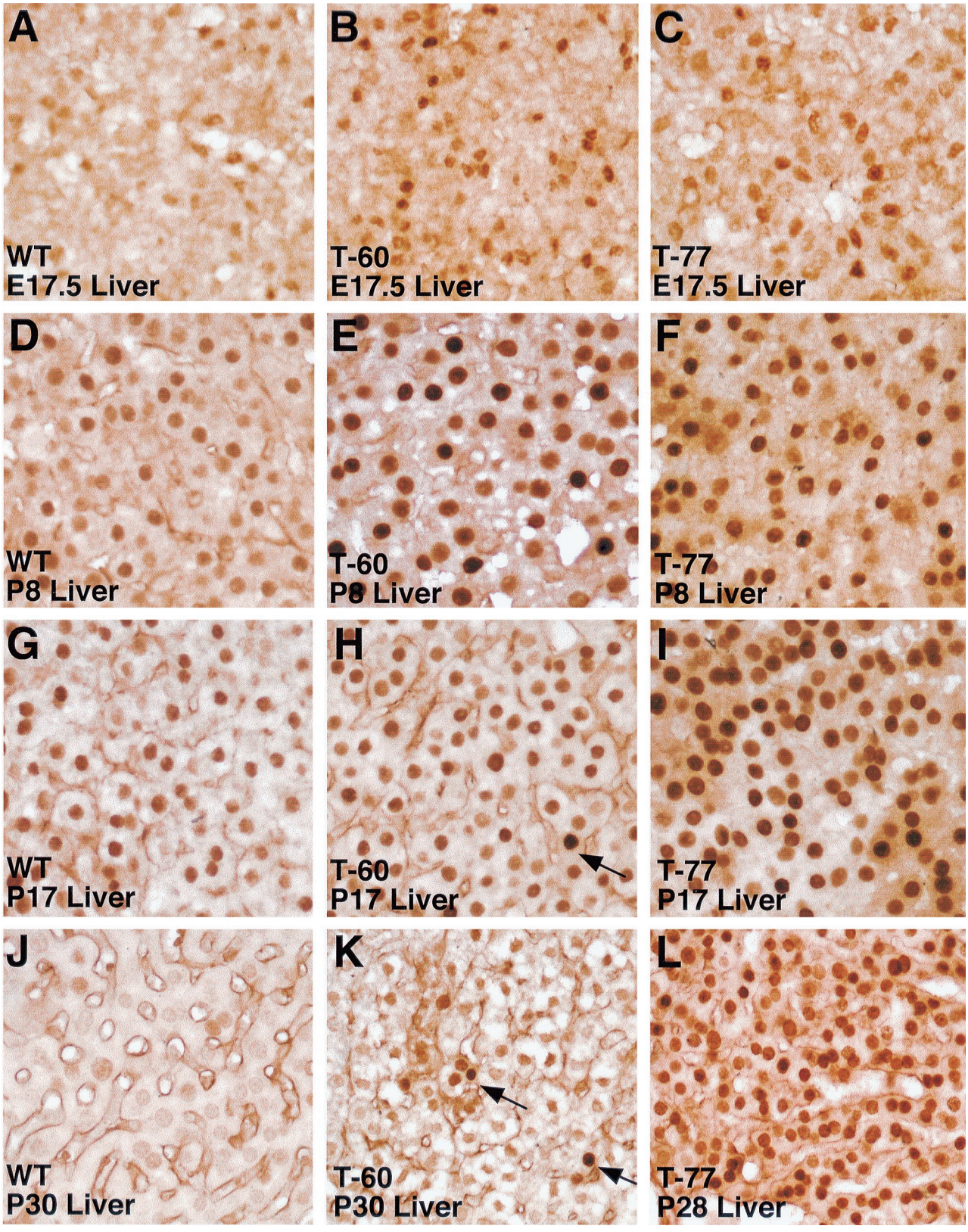

FIG. 2. Transgenic hepatocytes display an increase in HNF-3β protein expression. To determine HNF-3β protein expression, paraffin sections of wild-type (WT; A, D, G, and J) or transgenic (T-60 [B, E, H, and K] and T-77 [C, F, I, and L]) mouse liver were prepared from E17.5 embryos (A to C) or P8 (D to F), P17 (G to I), or P30 (J to L) mice and used for immunohistochemical staining with a monoclonal HNF-3β antibody (The University of Iowa Developmental Studies Hybridoma Bank). Hepatocyte expression of HNF-3β protein is more abundant in E17.5 (B and C) and P8 (E and F) transgenic liver than in wild-type liver (A and D). Continued abundant expression of HNF-3β protein in PI7 (I) and P30 (L) hepatocytes of the T-77 transgenic mice compared to wild-type liver (G and J) was seen. In T-60 transgenic mice, the number of hepatocytes displaying abundant expression of HNF-3β protein (indicated by arrows) diminishes by P17 (H) and is greatly reduced in P30 (K) liver.

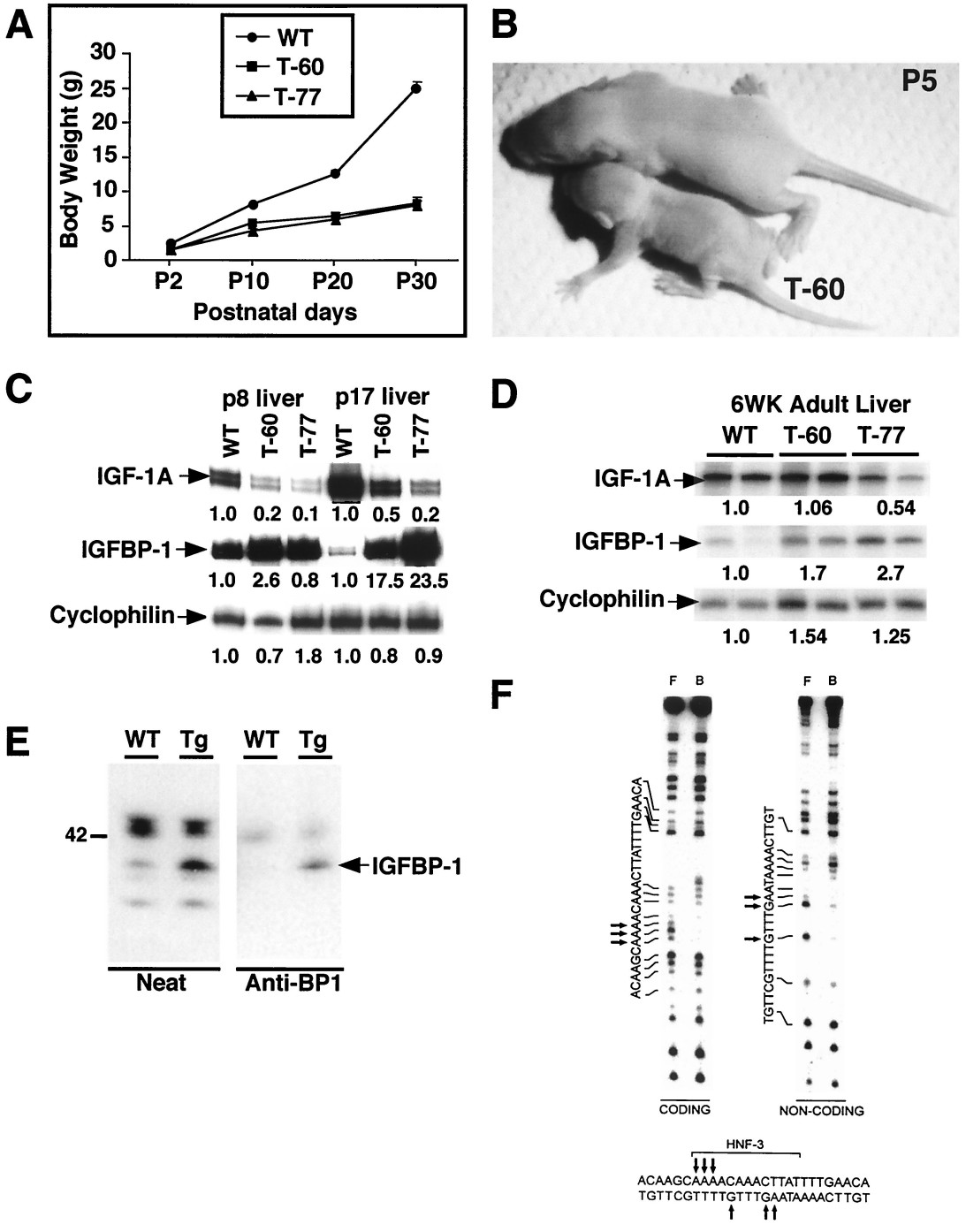

FIG. 3. Reduction in postnatal growth of TTR–HNF-3β transgenic mice coincides with increased liver expression of IGFBP-1. (A) Transgenic mice are retarded in postnatal growth. Shown graphically are the mean weights (n = 3, ± the standard error) of wild-type (WT) and transgenic (T-60 and T-77) mice at the indicated postnatal days (P2, P10, P20, and P30). (B) Photograph of P5 transgenic mouse (T-60) and wild-type littermate showing the reduction in transgenic mouse size. (C) Postnatal transgenic livers exhibit increased levels of IGFBP-1 mRNA expression. Total RNA was prepared from postnatal wild-type and transgenic mouse livers, and RNase protection assays were used to analyze for expression of IGF-1A, IGFBP-1, and cyclophilin. A cyclophilin RNase-protected band was used as a normalization internal control, and representative RNase protection assays displaying increased levels of IGFBP-1 mRNA and diminished expression of IGF-1A in postnatal transgenic livers compared to wild-type livers are shown. (D) Adult transgenic livers exhibit increased levels of IGFBP-1 mRNA expression. Shown are representative RNase protection assays from two distinct mice showing that postnatal transgenic livers express increased IGFBP-1 mRNA levels compared to wild-type livers. (E) Increased IGFBP-1 levels in T-77 transgenic line serum using Western ligand blotting and immunoprecipitation of IGFBP-1. Ligand blotting of circulating IGFBPs in 5-week-old wild-type and T-77 transgenic (Tg) mice (Neat labeled panel). IGFBPs in serum from wild-type and transgenic mice were separated by 4 to 20% nonreducing SDS-PAGE and then transferred to nitrocellulose and probed with [^{125}I]IGF-I prior to autoradiography at −70°C with enhancing screens. Immunoprecipitation of circulating IGFBP-1 (anti-BP-1 panel). Serum from wild-type and transgenic mice was incubated with specific anti-IGFBP-1 antibodies bound to Pansorbin beads. Bound proteins were eluted with Laemmli sample buffer and then loaded for SDS-PAGE and ligand blotting. Small amounts of 45-kDa IGFBP-3 bound nonspecifically to Pansorbin beads (67) and were detected in precipitates from both transgenic and wild-type sera. (F) Recombinant HNF-3β protein specifically binds to the insulin response element of the IGFBP-1 promoter. Methylation interference experiment demonstrates that methylation of the indicated G or A residues (arrows) of the IGFBP-1 promoter sequence at from −112 to −86 bp prevents binding of the recombinant HNF-3β protein.

TABLE 1. Postnatal transgenic and wild-type mouse serum analysis[a]

Strain	Mean level in serum ± SD of:						
	IGF-1 (ng/ml)	Bilirubin (mg/dl)	Bile acid (μmol/liter)	AST (U/liter)	ALT (U/liter)	AP (U/liter)	Glucose (mg/dl)
P8							
Wild type	ND[b]	0.95 ± 0.3	20 ± 4	428 ± 146	99 ± 35	464 ± 98	70 ± 24
T-77	ND	0.75 ± 0.2	20 ± 15	540 ± 209	154 ± 40	797 ± 98	39 ± 10
P17							
Wild type	487 ± 33	0.75 ± 0.4	19.5 ± 4.2	191 ± 44	15.8 ± 7.6	700 ± 62	32 ± 23
T-77	433 ± 63	0.55 ± 0.2	107 ± 99.5	403 ± 187	68 ± 23	572 ± 155	60.8 ± 17.2

[a] Mouse serum was isolated from postnatal day 17 (P17) TTR–HNF-3β transgenic and wild-type mice, and serum measurements were determined by Ani Lytics, Inc. The serum measurements are expressed as the mean and standard deviation from four mice. Abbreviations: aspartate aminotransferase (AST), alanine aminotransferase (ALT), alkaline phosphatase (AP).

[b] ND, not determined.

HNF-3β, HNF-3γ, and HNF-6 transcription factors when normalized to cyclophilin mRNA levels (Fig. 4A). Postnatal or adult livers of the T-77 transgenic line continued to display significant decreases in the expression of the HNF-3 and HNF-6 transcription factors and yet normal adult levels of HNF-4α, HNF-1α, C/EBPα, and C/EBPβ (Fig. 4B). We next generated a polyclonal antibody specific to the mouse HNF-6 protein, which allowed us to determine HNF-6 protein expression in the T-77 transgenic liver (see Materials and Methods). The specificity of the HNF-6 antibody was confirmed by its ability to alter the migration of the liver derived HNF-6 protein–DNA complex (supershift) in EMSA (Fig. 4C, lanes 3 and 4, indicated by arrows); this supershifted complex is not observed in preimmune serum (Fig. 4C, lane 2), and its formation is inhibited by the addition of the GST–HNF-6 fusion protein (antigen; Fig. 4C, lane 5). To measure hepatic HNF-6 protein levels, liver protein extracts were prepared from either wild-type or T-77 transgenic mice (5 weeks old) and used for Western blot analysis with affinity-purified HNF-6 antibody (Fig. 4D). The Western blot demonstrated that HNF-6 protein was not detectable in T-77 liver extracts (Fig. 4D, lanes 3 and 4) compared to wild-type liver protein (Fig. 4D, lanes 1 and 2), confirming reduction of hepatic HNF-6 protein levels in transgenic liver. These results suggest that reduced transcription of a subset of HNF-3 and HNF-6 target genes may contribute to the T-77 liver phenotype. By P17, the T-60 line has lost abundant hepatic expression of the HNF-3β transgene protein and hepatic expression levels of HNF-6 and HNF-3 recover (Fig. 4E and data not shown). These studies demonstrate that the T-77 transgenic liver expresses primarily the HNF-3β isoform, in contrast to normal hepatocyte expression of three HNF-3 isoforms, and exhibits significant reductions in HNF-6 levels.

Diminished hepatocyte glycogen storage in TTR–HNF-3β transgenic mouse livers. We next examined the possibility that transgenic mice were deficient in hepatocyte glycogen storage. Livers from postnatal wild-type and transgenic (T60 and T77) mice were stained for glycogen using the PAS reaction (glycogen is stained magenta) (14). Although the transgenic mouse livers possessed normal glycogen stores immediately postpartum (Fig. 5A to C), by P8 diminished hepatocyte glycogen levels were observed (Fig. 5D to F). By P17, however, the T-60 mice regained their ability to store hepatic glycogen (Fig. 5G and H), which occurs concomitant with the reduction in HNF-3β transgene protein expression (Fig. 2H). Postnatal T-77 transgenic livers continued to exhibit reduced hepatic glycogen levels compared to age-matched wild-type littermates or T-60 transgenic mice (Fig. 5G to L).

Because serum insulin and glucagon levels are normal in the TTR–HNF-3β transgenic mouse lines (Table 2), we hypothesize that hepatic glycogen depletion is due to altered expression of genes involved in glucose homeostasis. Indeed, P8 mice from both transgenic lines exhibited a reduction in hepatic expression of the HNF-3 target gene enzyme PEPCK (Fig. 6A) (72). PEPCK is the rate-limiting enzyme involved in gluconeogenesis, and its decreased levels are consistent with hepatocyte glycogen depletion (20). Furthermore, we observed a 50% decline in hepatic levels of glycogen synthase mRNA, which is also consistent with a reduction in hepatocyte glycogen storage. Interestingly, postnatal livers from both transgenic lines exhibited an increase in expression of the glucokinase gene, which remained elevated in P17 livers of the T-77 line (Fig. 6A and B). In P8 transgenic mice, we also observed a transient decrease in hepatic expression of the glycogen phosphorylase gene, which encodes the enzyme involved in glycogen mobilization. Normal hepatic expression of G6P was observed in all of the transgenic lines except in adult T-60 liver (Fig. 6). We observed elevated hepatic expression of the HNF-3–HNF-6 target gene enzyme PFK-2 (31, 32) in P8 and adult T-77 mice. Both P17 and adult T-77 liver continued to express reduced levels of PEPCK and glycogen synthase (GS) whereas its expression was restored in adult livers of T-60 mice which no longer expressed the *HNF-3*β transgene (Fig. 6B and C). This analysis suggests that hepatic expression of GS, PEPCK, and PFK-2 is altered in the T-77 line and that these changes are likely to contribute to the glycogen storage defects.

Elevated levels of bile acids and liver enzymes in serum in T-77 transgenic mice. In order to examine whether the HNF-3β transgene is influencing other liver functions, we determined the postnatal levels in serum of glucose, bilirubin, bile acids, and liver aminotransferases (Tables 1 and 2, ALT and AST) and alkaline phosphatase enzymes from the T-77 line. Serum parameters from P8 transgenic mice were similar to those from wild-type littermates, suggesting that postnatal transgenic liver function was normal (Table 1, T-77). This result supports the hypothesis that postnatal defects in hepatocyte glycogen storage were specific to elevated HNF-3β transgene expression rather than being caused by nonspecific effects from liver dysfunction. As early as P17, however, the T-77 transgenic mice began to exhibit elevated levels of bile acids and liver aminotransferase in serum, the latter of which suggests that some hepatocyte damage has occurred (Table 1) (22, 35). P17 transgenic mice displayed levels of alkaline phosphatase and bilirubin in serum identical to those of wild-type mice, indicating that there was no evidence of hepatic biliary damage or liver dysfunction. Despite hepatocyte glycogen storage defects, the postnatal T-77 transgenic mice were not hypoglycemic (Table 1). By 6 weeks of age, however, most of the T-77 transgenic mice were jaundiced, with serum bilirubin levels of >1 mg/dl (T-77J, Table 2), and they exhibited a 50-fold increase in levels of bile acids in serum compared to either wild-type littermates

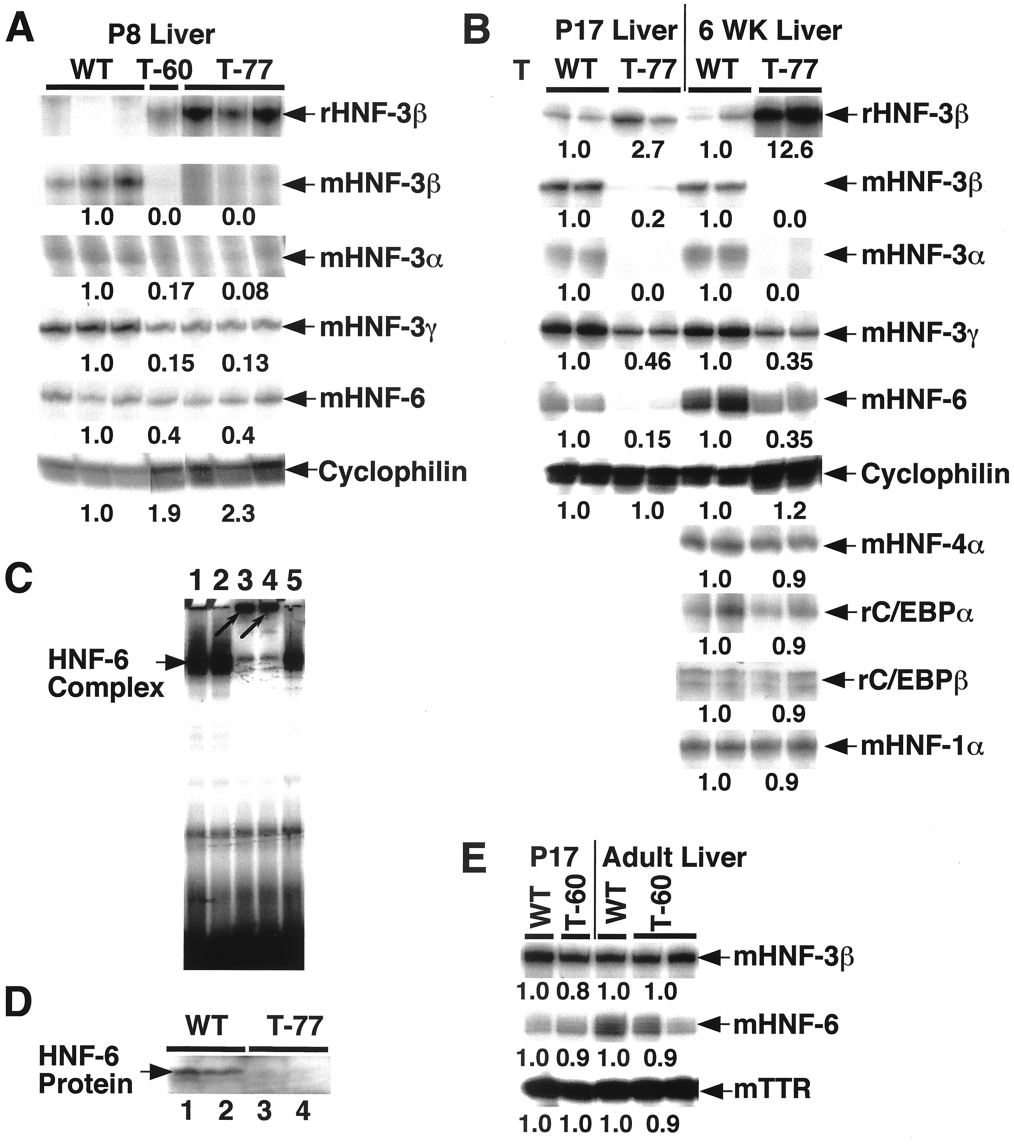

FIG. 4. T-77 transgenic liver exhibits reduced hepatic expression of HNF-3 isoforms and HNF-6. Total RNA was prepared from either P8, P17, or 6-week-old adult wild-type (WT) and transgenic mouse livers, and RNase protection assays were used to analyze for expression of rat HNF-3β, HNF-4α, C/EBPα, and C/EBPβ and mouse HNF-3α, HNF-3β, HNF-3γ, HNF-6, HNF-1α, and cyclophilin. To perform this RNase protection analysis, we used antisense RNA probes made to the untranslated portion of the mouse HNF-3α, HNF-3β, and HNF-3γ genes which would not cross-hybridize with the rat HNF-3β transgene. Shown are representative RNase protection assays performed on at least two wild-type and T-77 livers each from either P8 (A) or P17 and adult (6-week-old) mice (B). Panel A also shows the RNase protection assay for a single P8 liver from a T-60 mouse. The numbers below panels reflect the fold induction of transgenic liver mRNA levels compared to wild-type liver following normalization to the cyclophilin signal. (A and B) T-77 transgenic liver displays reduced mRNA levels of HNF-3α, HNF-3β, HNF-3γ, and HNF-6 but normal levels of C/EBPα, C/EBPβ, HNF-4α, and HNF-1α. P8 liver from the T-60 line shows similar decreases in mRNA levels of the HNF-3 and HNF-6 transcription factors. (C) HNF-6 antibody alters the migration of the HNF-6 protein–DNA complex. To examine specificity of the HNF-6 antibody, liver nuclear extracts were preincubated with buffer (lane 1), preimmune serum (lane 2), or 0.5 μl (lane 3) or 1 μl (lane 4) of HNF-6 antiserum and used for EMSA with the high-affinity HNF-6 DNA binding site (see Materials and Methods). The HNF-6 antibody altered or supershifted the migration of the hepatic HNF-6 protein–DNA complex (position indicated by arrow), and the supershifted complex formation was competed by inclusion of the GST–HNF-6 fusion protein in the preincubation step (lane 5). (D) HNF-6 protein expression is significantly decreased in T-77 transgenic mouse liver. HNF-6 protein expression was analyzed in liver protein extracts from either wild-type (lanes 1 and 2) or T-77 transgenic (lanes 3 and 4) mice by Western blot analysis using an affinity-purified HNF-6 antibody (see Materials and Methods). HNF-6 protein was not detectable in T-77 liver extracts compared to wild-type liver extracts. (Note that identical extracts were used for the HNF-3β Western blot in panel E.) (E) Normal hepatic levels of HNF-3 and HNF-6 in P17 and adult T-60 mice. RNase protection assay with P17 or 6-week-old mouse liver RNA from the T-60 line displays normal endogenous mouse expression of HNF-6 and HNF-3β transcription factors, which is consistent with diminished levels of HNF-3β transgene protein. The TTR band is used to normalize signals.

or the T-60 mice (Table 2). Although the levels of liver aminotransferase and alkaline phosphatase in serum were elevated in adult T-77 mice (6 weeks old; T-77J, Table 2), the observed increases in serum enzyme levels are not indicative of extensive biliary and hepatocyte damage. For example, mouse tail vein injection of adenovirus induces extensive liver hepatitis, and they displayed 10 times higher liver enzyme levels than those found in the adult T-77 mice (30). Moreover, a subset of adult T-77 transgenic mice exhibited proper liver function, as evidenced by normal serum bilirubin levels (nonjaundiced; T-77NJ, Table 2), but they still possessed elevated levels of liver enzymes and bile acids in serum.

Diminished hepatocyte expression of bile acid and phospholipid transporters in T-77 mice. One likely explanation for

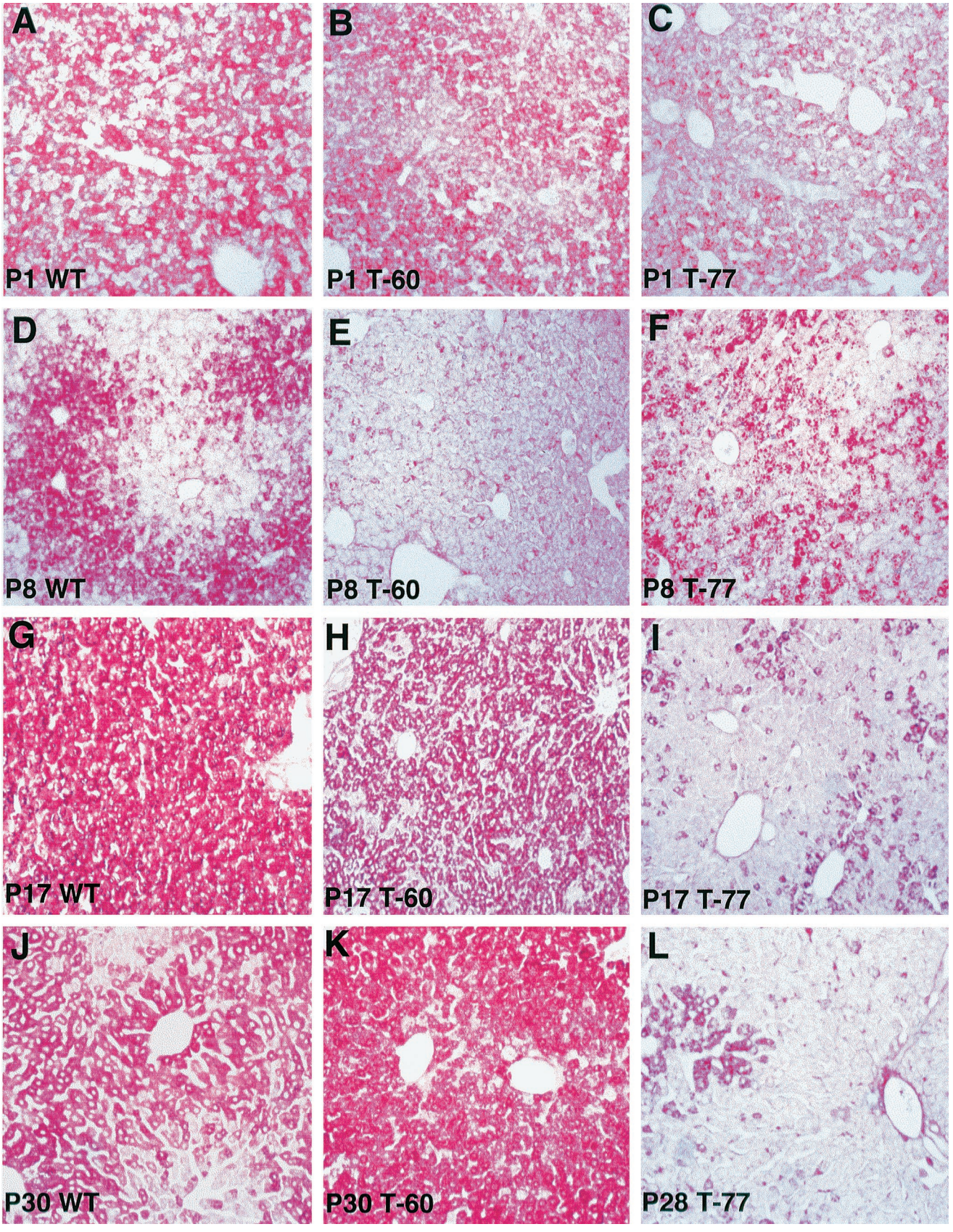

FIG. 5. Diminished hepatic glycogen storage in postnatal TTR–HNF-3β transgenic mice. Liver sections from wild-type (WT) and transgenic (T-60 and T-77) mice at P1 (A to C), P8 (D to F), P17 (G to I), P30 (J to K), or P28 (L) were stained with PAS (14) reagent to determine the hepatocyte glycogen content (stains magenta). (A to C) Transgenic and wild-type P1 livers store normal levels of glycogen. (D and E) Diminished hepatic glycogen storage in P8 transgenic liver. (G to I) Reduced hepatic glycogen storage in P17 transgenic liver of the T-77 but not the T-60 line, the latter of which correlates with a decline in HNF-3β transgene protein expression (Fig. 2). (J to L) Continued depletion of hepatic glycogen levels in P30 transgenic livers of the T-77 line.

TABLE 2. Serum analysis of T-60 and T-77 TTR–HNF-3β transgenic mice

Strain (age)	Mean level in serum ± SD of:								
	Bilirubin (mg/dl)	Bile acid (μmol/liter)	Bile acid change (fold)	AST (U/liter)	ALT (U/liter)	AP (U/liter)	Glucose (mg/dl)	Insulin (ng/ml)	Glucagon (pg/ml)
Wild type (adult)	0.15 ± 0.02	19.3 ± 10.5	Normal	96 ± 8	29 ± 8	88 ± 15	240 ± 22	ND	ND
T-60 (adult)	0.5 ± 0.1	24.7 ± 7.1	Normal	95.7 ± 28.3	27.7 ± 9.1	125 ± 79.8	196 ± 49.8	1.5 ± 1.0	39.7 ± 11.5
T-77 NJ (6 wk)	0.4 ± 0.1	333 ± 67	13.5	549 ± 78	316 ± 124	358 ± 240	195 ± 53	1.0 ± 0.4	55.5 ± 13.8
T-77 J (6 wk)	4.5 ± 2.6	1,226 ± 429	50	322 ± 87	196 ± 68	380 ± 162	138 ± 31	ND	ND
Reference range	0.00–0.90	15–50		72–288	24–140	45–222	124–262	0.40–2.40	25–90

[a] Mouse serum was isolated from TTR–HNF-3β transgenic mouse lines T-60 (no liver phenotype) and T-77. We analyzed T-77 transgenic mice at 6 weeks that were either nonjaundiced (T-77 NJ) or jaundiced (T-77 J) as evidenced by serum bilirubin levels of greater than 1.4 mg/dl. Shown is the fold change in bile acid levels in serum of the T-77PJ or T-77J transgenic compared to wild-type mice. The serum measurements are expressed as the mean and standard deviation from the following numbers of mice: T-60 (three mice), T-77 NJ (three mice), and T-77J (seven mice). Abbreviations are defined in Table 1, footnote *a*.

elevated levels of bile acids in serum in the T-77 mouse line is diminished hepatic expression of bile transporters which are involved in recycling serum bile acids (reabsorbed from the intestine) back into the hepatic biliary system (42, 64). Hepatocyte reuptake of serum-conjugated bile salts is mediated by the basolateral (sinusoidal) sodium-taurocholate cotransporter protein (Ntcp; Fig. 7A). Conjugated bile acids are then transported across the apical (canalicular) hepatocyte membrane into the bile canaliculi by the ATP-dependent bile transporter named sister of P-glycoprotein (Spgp) (42, 64). The basolateral multispecific organic anion-cation transporting polypeptide (Oatp) is involved in the reuptake of unconjugated bile salts, organic anion, and lipophilic compounds from the sinusoidal circulation (42, 64). RNase protection assays with T-77 postnatal and adult liver RNA reveal a substantial reduction in Ntcp expression, but its hepatic levels are only slightly reduced in T-60 mice (Fig. 7B and C). These results indicated that diminished hepatic expression of Ntcp precedes the increase in the levels of bile acids in serum, suggesting that its downregulation is specific to HNF-3β transgene levels. By contrast, mRNA levels of the canalicular Spgp bile transporter were normal in transgenic adult livers and exhibited only transient reductions in P8 transgenic livers (Fig. 7B and D). Expression of conjugated bilirubin canalicular multispecific organic anion transporter (cMoat) and Oatp was not significantly reduced in either postnatal or adult transgenic livers (Fig. 7B and D). These data suggest that diminished expression of Ntcp in the livers of postnatal T-77 transgenic mice is coincident with early onset of and persistence of increased bile acid levels in serum (Tables 1 and 2).

Another candidate gene involved in bile acid homeostasis is the canalicular multidrug resistance 2 (mdr2) P-glycoprotein, which transports intracellular phospholipids into bile secretion (Fig. 7A) and mediates protection of the biliary epithelial cells from bile injury. Homozygous null *Mdr2* mice display extensive damage to the liver parenchyma and biliary system and elevated levels of liver enzymes in serum and die postnatally of liver failure (62). Consistent with the mdr2 knockout phenotype, the increase in T-77 biliary and hepatocyte damage observed by 6 weeks of age is coincident with a 93% reduction in hepatic mdr2 mRNA levels, but its expression levels are normal in younger P17 transgenic livers (Fig. 7C and data not shown). These results suggest that reduction in the adult T-77 liver expression of mdr2 may contribute to the damage of hepatocytes and the biliary tree.

Transmission electron microscopy of T-77 transgenic livers shows bile canalicular damage and disruption of hepatocyte apical tight junctions. To examine the extent of abnormal hepatic architecture, wild-type and transgenic mouse livers were examined by light microscopy and processed for examination by transmission electron microscopy (see Materials and Methods). Light micrographs of P17 liver sections stained with toluidine blue displayed aberrant T-77 liver morphology (Fig. 8C) compared to its age-matched wild-type littermates (Fig. 8A). Although most bile canaliculi are intact in P17 livers from the T-77 line, several of them are visibly open to the basolateral domain (compare Fig. 8B and D, between arrowheads). The T-77 transgenic hepatocytes also contain large vacuoles, an increase in lipid-storing vesicles, and a complete absence of glycogen (Fig. 8C and D). Transmission electron microscopy of adult wild-type liver (Fig. 9 and 10A) shows the normal liver ultrastructure, with a single row of hepatocytes bordered on either basolateral side by sinusoids and on the apical side are tight junctions with intact bile canaliculi (Fig. 9 and 10A, arrowheads). In comparison with the wild-type adult liver, the ultrastructure of the T-60 hepatocytes is essentially normal, but they contain large vacuoles and the glycogen content appears increased and more dispersed throughout the cytoplasm (Fig. 10B). Transgenic hepatocytes from 3-month-old T-77 mice continue to display large vacuoles that often displace the hepatocyte nuclei, increased lipid-containing vesicles, and an absence of glycogen (Fig. 10C and D). The endothelium lining of the T-77 hepatic sinusoids is damaged, as evidenced by the lack of microvilli at the basolateral domain within the space of Disse, and the transgenic liver shows disruption of the bile canaliculi and basolateral tight junctions between hepatocytes (Fig. 10C, between arrows, and 10D). Despite the damage to the T-77 bile canaliculi, small and large intrahepatic bile ducts remain intact (Fig. 9, right panels and data not shown). Moreover, in a few areas of P17 and adult transgenic liver sections there is evidence of periportal fibrosis and an influx of immune cells (Fig. 8C and 10D). These studies demonstrate that, at 3 months of age, the T-77 adult livers display injury to the bile canaliculi and disruption of hepatocyte tight junctions.

DISCUSSION

Homozygous null *Hnf3*β mice die in utero at 10 days postcoitum, thereby precluding examination of the in vivo function of HNF-3β in the regulation of hepatocyte-specific gene transcription (1, 73). To perform the study reported here, we created transgenic mice that display increased hepatocyte HNF-3β levels and then assessed the consequences of elevated HNF-3β on hepatocyte-specific gene regulation. The transgenic mice are smaller than their wild-type littermates and exhibit elevated levels of bile acids in serum and an absence of hepatic glycogen storage. We show that these defects are coincident with diminished expression of hepatocyte genes involved in glucose homeostasis (PEPCK and glycogen synthase) and sinusoidal bile acid uptake (Ntcp). Retarded postnatal

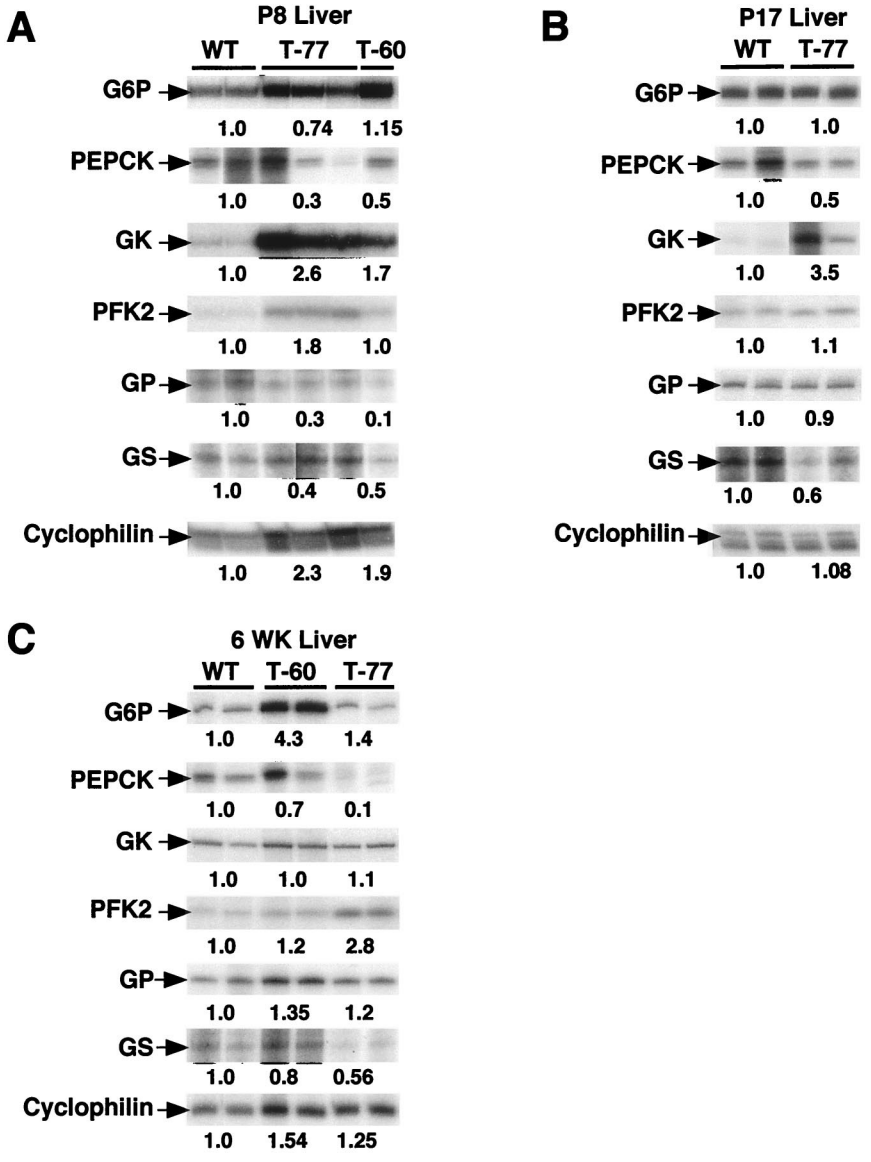

FIG. 6. Hepatocyte glycogen storage defect in T-77 transgenic livers coincides with reduced expression of the gluconeogenic enzyme PEPCK. (A) Postnatal T-77 transgenic liver exhibits reduced expression of glucose homeostasis genes. Total RNA was prepared from wild-type (WT) and transgenic mouse liver (P8, P17, and 6-week-old adults), and RNase protection assays were used to analyze the expression of the gluconeogenic PEPCK and G6P, glucokinase (GK), PFK-2, glycogen phosphorylase (GP), glycogen synthase (GS), and cyclophilin. A cyclophilin RNase-protected band was used as a normalization internal control. Indicated below each panel is the normalized fold induction of transgenic liver expression compared to wild-type liver. Shown are representative RNase protection assays using two distinct transgenic or wild-type livers. (A) P8 transgenic livers from either the T-60 or T-77 transgenic line express diminished mRNA levels of GS and PEPCK and exhibit elevated levels of glucokinase and PFK-2 mRNA. (B) Diminished GS and PEPCK and elevated glucokinase mRNA levels continue in P17 transgenic liver from the T-77 line. (C) Diminished GS and PEPCK and elevated PFK-2 mRNA levels continues in adult transgenic liver from the T-77 line.

growth is coincident with an increase in hepatic IGFBP-1 levels, which limits the biological effects of IGFs in the circulation and in target tissues. The observed phenotypes may also result from diminished expression of the HNF-3α,-3β, -3γ, and -6 transcription factors, suggesting that increased HNF-3β levels disrupted the normal hepatocyte expression of liver transcription factors. We were able to determine that these changes in hepatocyte gene expression are specific to the HNF-3β transgene because they were also observed in P8 livers of the T-60 line when those hepatocytes were still expressing the HNF-3β transgene protein. Furthermore, transgenic liver displayed sustained, normal hepatic expression levels of genes involved in bile acid transport (Spgp and Oatp), glucose homeostasis (G6P and GP), and IGFBP-3, as well as the other liver transcription factors HNF-1α, HNF-4α, C/EBPα, and C/EBPβ. We can also conclude that this altered hepatic gene expression is not due to liver hepatitis because transgenic hepatocytes were not proliferating (data not shown), nor did they exhibit changes in C/EBPα, C/EBPβ, and Spgp mRNA levels, which change dramatically in regenerating and acute-phase livers (11, 48, 69). Furthermore, the levels of liver enzymes in the serum of adult T-77 transgenic mice were 10-fold lower than those found in adenovirus-infected mice with hepatitis (30).

The TTR–HNF-3β transgenic mouse phenotype involves disruption of the HNF-3 isoforms and HNF-6 transcription factors. Our transgenic mouse analysis demonstrates that the T-77 transgenic liver expresses primarily the HNF-3β isoform, instead of the normal hepatocyte expression of all three HNF-

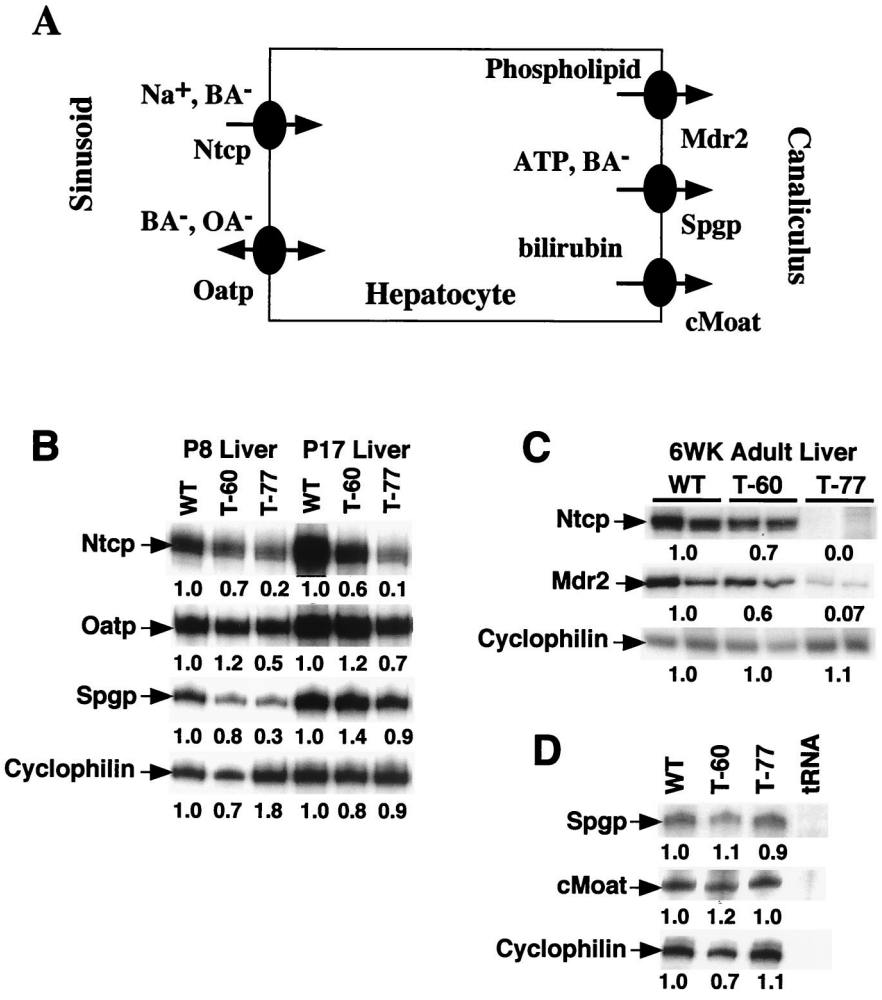

FIG. 7. T-77 transgenic liver exhibits reduced hepatic expression of sinusoidal bile acid transporters and canalicular bile phospholipid transporters. (A) Schematic representation of the sinusoidal and canalicular bile acid, organic acid phospholipid, and bilirubin transporter proteins. Shown is the sinusoidal (basolateral) Ntcp, the Oatp, and the canalicular (apical) mdr2 P-glycoprotein phospholipid transporter, Spgp ATP-dependent bile transporter (also known as bile salt export pump), and bilirubin canalicular multispecific organic anion transporter (cMoat; also known as cmrp2). The double arrow indicates that Oatp can transport organic anions in both directions. Total RNA was prepared from P8, P17, and adult wild-type and transgenic mouse livers, and RNase protection assays were used to analyze for expression of Ntcp, Oatp, Spgp, Mdr2, cMoat, and cyclophilin. Indicated below each panel is the normalized fold induction of transgenic liver expression compared to wild-type liver. (B) Decreased Ntcp mRNA levels in postnatal T-77 transgenic livers. (C) Adult T-77 transgenic liver (6 weeks old) exhibited diminished expression of Ntcp and Mdr2. (D) Adult T-77 transgenic liver exhibited normal levels of Spgp and cMoat mRNAs.

3 isoforms. The presence of the HNF-3β protein alone in transgenic hepatocytes may influence the transcription of a subset of genes in which the DNA regulatory region is recognized by a distinct HNF-3 isoform, as has been observed in TTR regulatory sequences (28, 58). One potential mechanism mediating diminished expression of the endogenous HNF-3 genes involves the direct binding of the HNF-3β transgene protein to its autoregulatory sites in the HNF-3α and HNF-3β promoter regions (45, 46). In this model, the HNF-3 binding site may function to diminish HNF-3α and HNF-3β gene transcription in response to an excess of HNF-3β protein. The transgenic livers also display significant reductions in HNF-3γ expression, but its promoter has not been characterized in detail, and we are therefore unable to propose a model for its diminished hepatic expression. In postnatal T-60 and T-77 transgenic livers, we also observed a significant decrease in HNF-6 expression, suggesting that we have created a hepatocyte-specific ablation of HNF-6. Although we do not know whether HNF-3β mediates a direct or indirect downregulation of HNF-6 expression, it is likely that reduced transcription of the HNF-6 target gene contributes to the T-77 liver phenotype. Moreover, because HNF-6 is known to transcriptionally activate the HNF-3β promoter (29, 52, 57), another possibility is that diminished HNF-6 expression is contributing to reduced expression of the endogenous mouse HNF-3β gene. Previous cotransfection studies demonstrated that HNF-6 is also capable of stimulating HNF-4α promoter activity, suggesting that HNF-6 may regulate transcription of the HNF-4α gene in developing and adult livers (29). In spite of diminished hepatic levels of HNF-6 in the T-77 mice, adult hepatic expression of HNF-4α was not affected. This result suggests that the HNF-6 to HNF-4α regulatory pathway is not essential for the maintenance of adult hepatic HNF-4α expression in vivo.

Which of the HNF-3 target genes are involved in retarded postnatal growth and defects in hepatocyte glycogen storage? IGFBP-1 gene expression is activated by the winged helix transcription factor, Fkhr, which recognizes the IRE in its promoter region (6, 19). IGFBP-1 promoter activation is negatively regulated by insulin through Akt (protein kinase B)-mediated phosphorylation of fkhr, which causes cytoplasmic

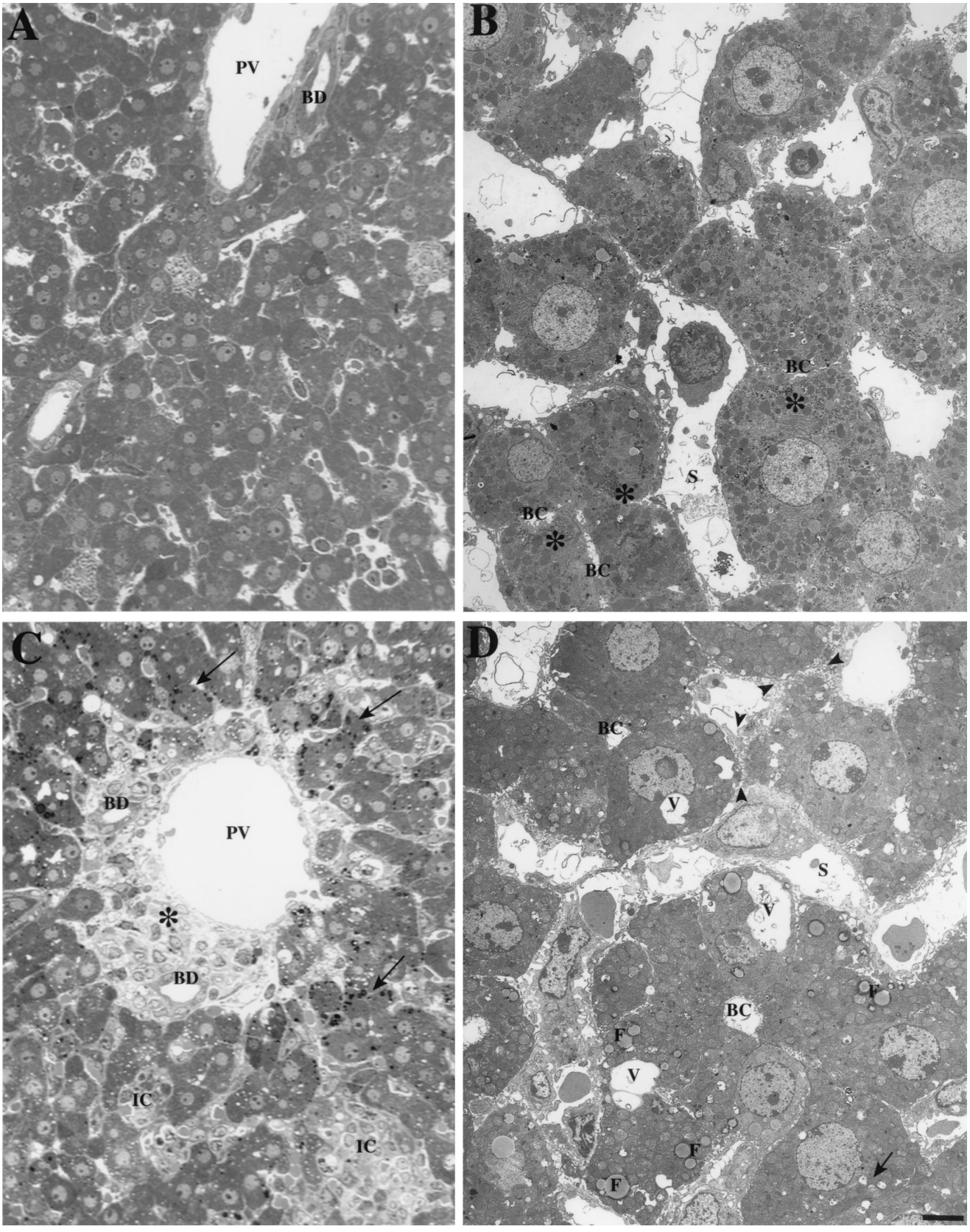

FIG. 8. Morphology and ultrastructure of livers from P17 wild-type and T-77 transgenic mice. Livers were obtained from P17 mice and processed for transmission electron microscopy as described in Materials and Methods. (A) Light micrograph of toluidine blue-stained 300-μm section of P17 wild-type mouse liver shows normal architecture with intact bile ducts (BD). (B) The ultrastructure from these wild-type livers also displays normal architecture with intact bile canaliculi (BC) at the apical membrane domain, abundant glycogen (*) in the cytoplasm, and hepatic sinusoidal (S) plate structure. (C) Light micrograph of toluidine blue-stained

retention of fkhr protein. In the current study, reduction in postnatal transgenic mouse growth is coincident with stimulated hepatic expression of the IGFBP-1 gene. Methylation interference experiments demonstrate that HNF-3β protein specifically binds the IGFBP-1 promoter region, and previous NIH 3T3 cell cotransfection studies showed that retention of this HNF-3 binding sequence is necessary to mediate HNF-3β activation of IGFBP-1 promoter expression (66). The elevated hepatic IGFBP-1 levels in postnatal T-60 and T-77 transgenic mice confirm these transfection studies by demonstrating that HNF-3β is also able to activate IGFBP-1 expression in vivo. Furthermore, we demonstrated that elevated hepatic expression of IGFBP-1 resulted in a significant increase in levels of IGFBP-1 in transgenic mouse serum (Fig. 3E). Although IGFBP-3 is the predominant serum carrier protein for IGF-1 (55), increased expression of IGFBP-1 in transgenic mice causes significant reductions in postnatal growth, confirming its role in regulating the biological activity of IGFs (16, 51). The increase in hepatic expression and the resulting increase in serum IGFBP-1 levels therefore provides a plausible explanation for the reduction in postnatal growth of the TTR–HNF-3β transgenic mouse lines. Paradoxically, despite reduced hepatic expression of IGF-1 in postnatal T-77 transgenic mice, they displayed normal levels of IGF-1 protein in serum. One possible explanation for this result resides in the ability of increased levels of IGFBP-1 in serum to mediate the stabilization of serum IGF-1 protein (18). Furthermore, recent conditional knockout mouse studies demonstrated that, although hepatocyte-specific ablation of the IGF-1 gene caused a 75% reduction in serum IGF-1 levels, the mice still exhibited normal postnatal growth (61, 75). These studies support the hypothesis that reduced postnatal growth of the TTR–HNF-3β transgenic mice is due to increased hepatic IGFBP-1 expression, with no reduction in serum IGF-1.

The TTR–HNF-3β transgenic mouse livers possessed normal glycogen stores immediately postpartum, but their hepatocyte glycogen levels were diminished by P8. This result suggests that postnatal transgenic hepatocytes are unable to maintain normal glycogen levels. The decreased hepatocyte glycogen storage capability of transgenic livers is not due to liver dysfunction, because glycogen depletion was evident in P8 livers when the transgenic mice exhibited normal levels in serum of bilirubin, bile acids, and liver enzymes. The glycogen storage defect is coincident with diminished expression of the PEPCK gene, which is activated in postnatal liver and is the rate-limiting enzyme in the gluconeogenic pathway (20). Although the HNF-3β protein is known to activate expression of the PEPCK promoter region (72), we observed that increased hepatocyte HNF-3β levels mediate decreases in postnatal PEPCK mRNA levels. A 50% reduction in hepatic PEPCK mRNA levels was observed in homozygous null HNF-3γ mice even though they exhibited elevated hepatic expression of the other two HNF-3 isoforms (24). Our study supports this result in that normal expression of PEPCK requires the HNF-3γ isoform and increased HNF-3β levels are insufficient to sustain normal hepatic levels of PEPCK mRNA. Furthermore, we also observed a 50% decline in hepatic expression of the glycogen synthase gene, which is consistent with diminished glycogen storage in transgenic hepatocytes. Similar to the TTR–HNF-3β transgenic mice, the *C/EBPα*$^{-/-}$ mice exhibit postnatal defects in hepatic glycogen storage resulting from reduced induction of hepatic expression of PEPCK and glycogen synthase (70). We also noted significant increases in postnatal transgenic expression of glucokinase, suggesting that glucokinase transcription may be regulated by HNF-3β protein. Consistent with this possibility, the human glucokinase promoter contains a consensus HNF-3 binding site (797/−784; AcTATTGACTgA). Postnatal and adult transgenic liver exhibited elevated PFK-2 mRNA levels, which confirms its transcriptional regulation by HNF-3 (31). Because PFK-2 is a bifunctional enzyme whose products influence gluconeogenesis, its increase in transgenic hepatocytes may also contribute to diminished hepatic glycogen stores (23). More recently, HNF-6 protein has been shown to inhibit glucocorticoid hormone induction of PFK-2 gene transcription through direct interaction with the glucocorticoid receptor DNA-binding domain (47). Another possibility is that diminished HNF-6 protein levels in the T-77 transgenic liver may lead to elevated glucocorticoid induction of the PFK-2 gene and contribute to its increased hepatic expression.

Diminished expression of hepatic Ntcp and mdr2 in T-77 transgenic mice leads to elevated serum bile acids and extensive liver damage, respectively. Hepatocytes synthesize and secrete bile acids which are stored in the gallbladder and released into the intestine to emulsify fat for digestion (42). Approximately 90% of the bile acids are reabsorbed from the ileum, transported through the hepatic vein to the sinusoidal circulation, and recycled back into the hepatic biliary system by hepatocyte bile acid transporter proteins (13, 63). The majority of hepatocyte reuptake of bile salts from the hepatic sinusoidal circulation is mediated by the basolateral Ntcp (42). Bile is then transported against a concentration gradient across the apical hepatocyte membrane into the bile canaliculi by the ATP-dependent Spgp bile transporter (17, 42). In P8 transgenic T-77 mice, we show that abrogated hepatic expression of the sinusoidal bile acid transporter protein, Ntcp, precedes elevated levels of bile acids in serum. This result indicates that downregulation of hepatic Ntcp levels is likely due to the HNF-3β transgene rather than increased serum levels of bile acids (26). The T-60 line exhibited no increases in serum bile acid levels (data not shown). A plausible explanation is found in our observation that a transient decrease in P8 hepatic expression of Ntcp is insufficient to elicit elevated levels of bile acids in the serum of T-60 mice. These results strongly support the hypothesis that continued downregulation of hepatic Ntcp levels in the T-77 line diminishes bile acid reuptake and contributes to the elevated levels of bile acids in serum. Consistent with the role of HNF-6 in regulating Ntcp expression, the Rat Ntcp promoter region contains a consensus HNF-6 binding site (−758/−770; TTTATTGACTgTT) which is recognized by recombinant HNF-6 protein and mediates its transcriptional activation by HNF-6 (F. M. Rausa, S. Karpen, and R. H. Costa, unpublished results). These results suggest that diminished hepatic expression of HNF-6 may also contribute to reduced transcription of Ntcp in the T-77 liver. Coincident with increased levels of bile acids in the serum of T-77 mice, we observed an 80% decrease in P17 hepatic mRNA levels of cholesterol 7α-hydroxylase (Cyp7A; data not shown), the rate-limiting enzyme involved in the synthesis of bile acids from cholesterol (5).

300-μm section of P17 liver from the T-77 transgenic line shows bile ducts (BD) that appear normal and intact, but some periportal fibrosis is evident (*). Many hepatocytes in T-77 transgenic livers display lipid accumulation (arrows), and some areas are filled with immune cells (IC). (D) A high-magnification view of P17 transgenic liver from the T-77 line displays aberrant morphology. Many hepatocytes display large vacuoles (V), as well as numerous smaller vacuoles (arrows), throughout the cytoplasm. Although most bile canaliculi (BC) are intact, and several are visibly open (between arrowheads) to the basolateral domain. Also of note is the complete absence of glycogen but an increase in lipid-storing vesicles (F) in the hepatocytes. A and C, × 40 magnification; B and D, bar = 5 μm.

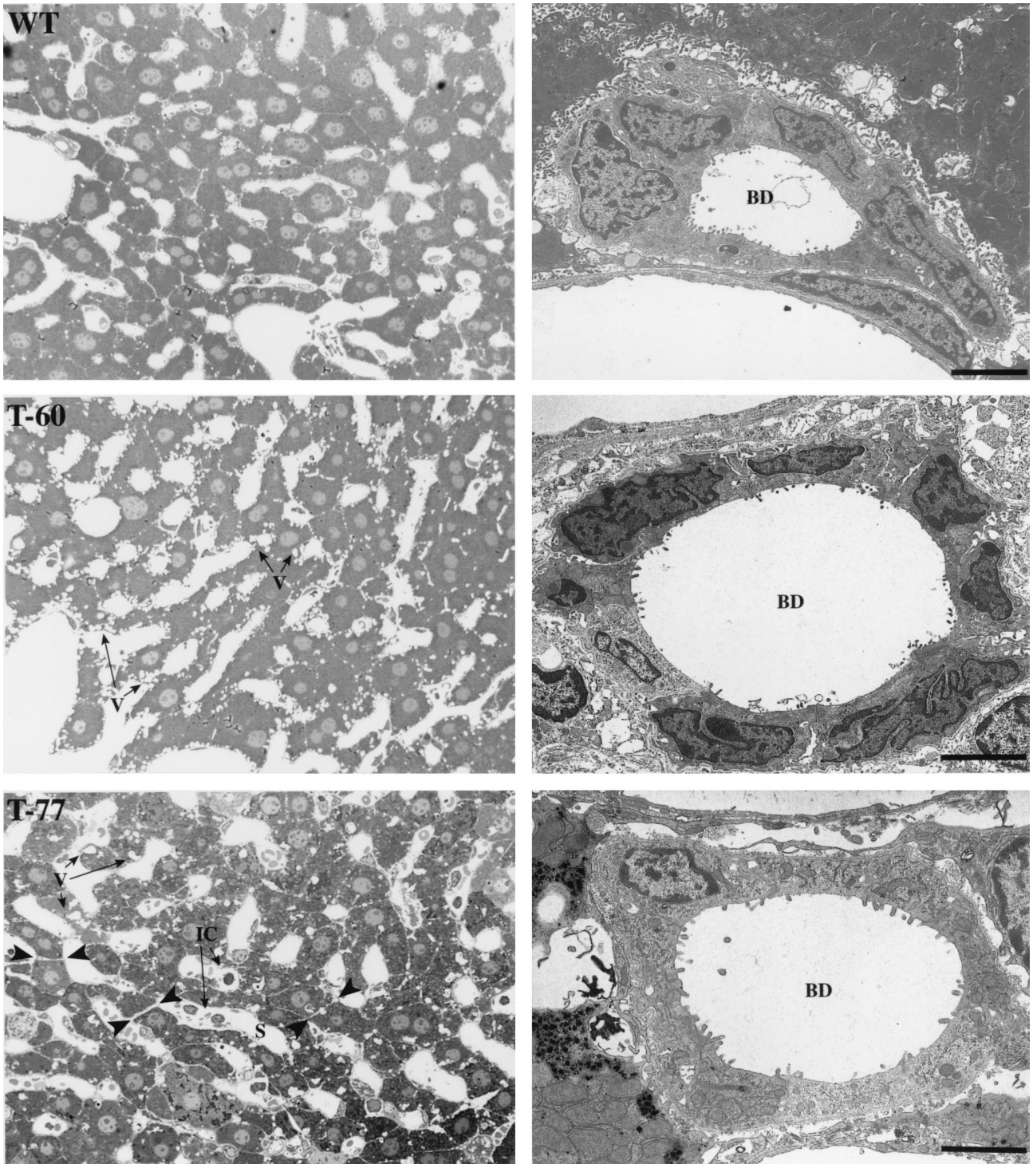

FIG. 9. Comparative analysis of adult wild-type (WT), T-60, and T-77 liver morphology and bile duct ultrastructure. Toluidine blue-stained 300-μm sections of adult livers from 3.5-month-old mice were examined for general morphology (left panels). Wild-type livers display normal architecture. Hepatocytes in the T-60 transgenic livers show many submembrane vacuoles (V) closely apposed to both the apical and basolateral plasma membranes. Livers from T-77 transgenic mice display distended, as well as disrupted, bile canaliculi (between arrowheads), hepatocytes with large vacuoles (V), and some areas with immune cells (IC) within the sinusoids (S). Representative transmission electron micrographs of small bile ducts from each mouse strain (right panels; wild type, T-60, and T-77) show that bile ducts are normal. Left-panel magnifications, ×20. Right panel bars: WT and T-60, 4 μm; T-77, 2 μm.

Because bile acids are the endogenous ligands for the farnesoid X receptor (26, 36), which mediates transcriptional repression of the Cyp7A gene, we were unable to determine whether diminished hepatic expression in T-77 mice is due to an indirect effect of increased levels of bile acids in hepatocytes through import by the sinusoid multispecific organic anion-cation-transporting polypeptide. Moreover, we observed normal hepatic expression of Spgp in the T-77 mice, allowing

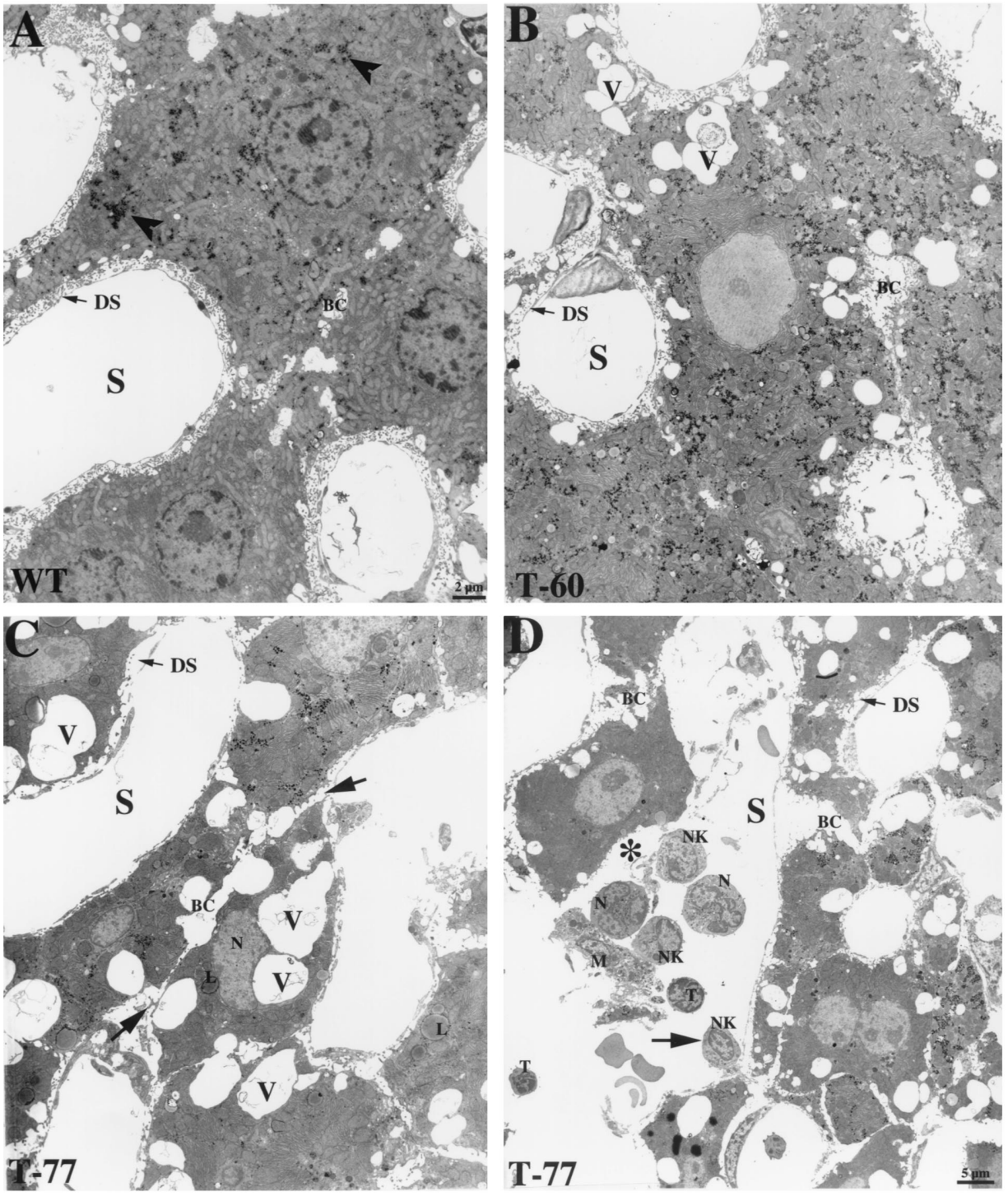

FIG. 10. Ultrastructure of adult livers from wild-type (WT) and T-60 and T-77 transgenic mice. Livers were obtained from 3.5-month-old mice and processed for transmission electron microscopy as described in Materials and Methods. (A) Wild-type liver displays typical liver ultrastructure with a single row of hepatocytes bounded on either basolateral side by sinusoids (S), and glycogen is evident throughout the hepatocytes (arrowheads). Intact bile canaliculus (BC) is evident between the apical membrane domains of the hepatocytes and is surrounded by a ring of tight junctions. (B) T-60 transgenic mouse liver displays typical liver ultrastructure similar to that observed in the wild-type liver. However, in many hepatocytes, large vacuoles (V) are apparent just under the plasma membrane in both the apical and the basolateral domains and exhibits an increase in glycogen content that is more dispersed throughout the cytoplasm compared to wild-type liver. (C) Liver from a 3-month-old adult T-77 transgenic mouse displays many striking abnormalities compared to liver from a wild-type or T-60 transgenic mouse. The hepatocytes are filled with large vacuoles (V) that often displace the nucleus (N) of the hepatocyte. The bile canaliculi are often not intact and patent to the basolateral membrane domain of the hepatocyte (between arrows), suggesting leakage of bile into the sinusoidal blood. Additionally, a greater number of lipid containing vesicles (L), but less glycogen storage, are evident in this line. (D) In other areas of the adult T-77 liver lobule, infiltrating immune cells, including natural killer cells (NK), neutrophils (N), T cells (T), and macrophages (M), are coalescing within a sinusoid (S). Bile canaliculi (BC) are not intact and are open to the sinusoid, and the sinusoidal endothelial cell adjacent to the immune cells is destroyed (*). One natural killer cell is observed migrating between two endothelial cells into the parenchymal cells below (arrow). In panels C and D, hepatocytes in T-77 transgenics do not possess microvilli at the basolateral domain within the space of Disse (DS), indicating sinusoidal damage. A to C, bar = 2 μm; D, bar = 5 μm.

continued transport of de novo hepatocyte bile into the biliary system and preventing complete hepatic cholestasis.

The T-77 transgenic line was noted to develop liver disease by 6 weeks of age, as evidenced by the development of jaundice (elevated serum bilirubin levels). Preliminary analysis of P22 transgenic mice (T-77) indicates that the hepatic expression of the bilirubin-conjugating enzyme UDP-glucuronosyltransferase is significantly diminished, suggesting that the jaundiced phenotype is a specific effect of the HNF-3β transgene (X. Wang, D. Hughes, and R. H. Costa, unpublished results). Furthermore, adult transgenic mice display liver damage, as indicated by elevated liver enzymes in serum and disruption of normal liver architecture. This adult transgenic phenotype is coincident with extinguished expression of the phospholipid transporter protein, mdr-2, which functions to protect the biliary epithelial cell lining. Homozygous *Mdr2* null mice display extensive damage to hepatocytes and bile canaliculi, exhibit elevated levels of liver enzymes in serum, and die postnatally of liver failure (62). The increase in bile acid levels in serum and diminished phospholipid transport into bile secretion may lead to disruption of the hepatocyte tight junctions required to separate the contents of the bile canaliculi from the sinusoidal circulation. Transmission electron microscopy of adult transgenic liver from 3-month-old T-77 mice confirms hepatocyte and bile canalicular damage leading to disruption of apical tight junctions between hepatocytes. We believe that the combination of elevated bile acids in serum and diminished phospholipid transport into the bile secretion leads to liver damage and eventual liver failure. Furthermore, a portion of the elevated bilirubin and bile acid levels in the serum of the T-77 transgenic mouse line may be the result of leakage from damaged hepatocytes or bile canaliculi into the sinusoidal circulation. More recent studies have also demonstrated that increased bile acid levels in mdr2-deficient mice result in a decline in Ntcp protein levels (26). This result suggests that reduced hepatic expression of mdr2 in adult T-77 mice may also contribute to further increases in bile acid levels in the serum of adult transgenic mice.

In summary, increased hepatocyte expression of HNF-3β in transgenic mice caused postnatal growth retardation, diminished liver glycogen storage, elevated bile acids in serum, and subsequent damage to the adult liver parenchyma. We show that these defects are coincident with diminished expression of genes involved in gluconeogenesis, the sinusoidal reuptake of bile acids by hepatocytes, and biliary homeostasis. Furthermore, the retarded growth phenotype is coincident with elevated hepatic expression of IGFBP-1, which limits stimulation of postnatal growth by serum IGF proteins in target tissues. We also show that TTR–HNF-3β transgenic livers express diminished levels of endogenous HNF-3 and HNF-6 transcription factors, suggesting that changes in transcription of both HNF-3 and HNF-6 target genes contribute to this liver phenotype.

ACKNOWLEDGMENTS

We thank K. Wang for her expert assistance in generating the transgenic mice, Raul Lacson for his technical assistance in performing the methylation interference studies, and Xiaohue He for performing Western ligand blotting and immunoprecipitation studies of IGFBPs. We also thank T. A. Van Dyke for providing us the −3-kb TTR minigene expression plasmid and Pradip Raychaudhuri, Ai Xuan Holterman, Richard Green, Saul Karpen, and Xinhe Wang for critically reading the manuscript. The HNF-3β monoclonal antibody (4C7) developed by T. M. Jessell and S. Brenner-Morton was obtained from the Developmental Studies Hybridoma Bank developed under the auspices of the NICHD and maintained by the Department of Biological Sciences, The University of Iowa, Iowa City, Iowa.

This work was supported by National Institutes of Health grants R01 GM43241-10 (R.H.C.), RO1 DK41430 (T.G.U.), and RO1 CA76541 (D.B.S.) and by an American Liver Foundation Liver Scholar Grant (D.B.S.) and the Department of Veterans Affairs Merit Review Program (T.G.U.).

F.M.R., Y.T., and H.Z. contributed equally to this study.

REFERENCES

1. **Ang, S. L., and J. Rossant.** 1994. HNF-3β is essential for node and notochord formation in mouse development. Cell **78:**561–574.
2. **Ang, S. L., A. Wierda, D. Wong, K. A. Stevens, S. Cascio, J. Rossant, and K. S. Zaret.** 1993. The formation and maintenance of the definitive endoderm lineage in the mouse: involvement of HNF3/forkhead proteins. Development **119:**1301–1315.
3. **Baker, J., J. P. Liu, E. J. Robertson, and A. Efstratiadis.** 1993. Role of insulin-like growth factors in embryonic and postnatal growth. Cell **75:**73–82.
4. **Cereghini, S.** 1996. Liver-enriched transcription factors and hepatocyte differentiation. FASEB J. **10:**267–282.
5. **Chiang, J. Y. L.** 1998. Regulation of bile acid synthesis. Front. Biosci. **3:** D176–D193.
6. **Cichy, S. B., S. Uddin, A. Danilkovich, S. Guo, A. Klippel, and T. G. Unterman.** 1998. Protein kinase B/Akt mediates effects of insulin on hepatic insulin-like growth factor-binding protein-1 gene expression through a conserved insulin response sequence. J. Biol. Chem. **273:**6482–6487.
7. **Cirillo, L. A., C. E. McPherson, P. Bossard, K. Stevens, S. Cherian, E. Y. Shim, K. L. Clark, S. K. Burley, and K. S. Zaret.** 1998. Binding of the winged-helix transcription factor HNF3 to a linker historic site on the nucleosome. EMBO J. **17:**244–254.
8. **Clark, K. L., E. D. Halay, E. Lai, and S. K. Burley.** 1993. Co-crystal structure of the HNF-3/fork head DNA-recognition motif resembles histone H5. Nature **364:**412–420.
9. **Cooper, A. D., J. Chen, M. J. Botelho-Yetkinler, Y. Cao, T. Taniguchi, and B. Levy-Wilson.** 1997. Characterization of hepatic-specific regulatory elements in the promoter region of the human cholesterol 7α-hydroxylase gene. J. Biol. Chem. **272:**3444–3452.
10. **Costa, R. H., D. R. Grayson, and J. E. Darnell, Jr.** 1989. Multiple hepatocyte-enriched nuclear factors function in the regulation of transthyretin and α1-antitrypsin genes. Mol. Cell. Biol. **9:**1415–1425.
11. **Diehl, A. M.** 1998. Roles of CCAAT/enhancer-binding proteins in regulation of liver regenerative growth. J. Biol. Chem. **273:**30843–30846.
12. **Dufort, D., L. Schwartz, K. Harpal, and J. Rossant.** 1998. The transcription factor HNF3β is required in visceral endoderm for normal primitive streak morphogenesis. Development **125:**3015–3025.
13. **Erlinger, S.** 1996. Review article: new insights into the mechanisms of hepatic transport and bile secretion. J. Gastroenterol. Hepatol. **11:**575–579.
14. **Frederiks, W. M., F. Marx, and C. J. Van Noorden.** 1987. Quantitative histochemical assessment of the heterogeneity of glycogen phosphorylase activity in liver parenchyma of fasted rats using the semipermeable membrane technique and the PAS reaction. Histochem. J. **19:**150–156.
15. **Galarneau, L., J. F. Pare, D. Allard, D. Hamel, L. Levesque, J. D. Tugwood, S. Green, and L. Belanger.** 1996. The α1-fetoprotein locus is activated by a nuclear receptor of the *Drosophila* FTZ-F1 family. Mol. Cell. Biol. **16:** 3853–3865.
16. **Gay, E., D. Seurin, S. Babajko, S. Doublier, M. Cazillis, and M. Binoux.** 1997. Liver-specific expression of human insulin-like growth factor binding protein-1 in transgenic mice: repercussions on reproduction, ante- and perinatal mortality and postnatal growth. Endocrinology **138:**2937–2947.
17. **Gerloff, T., B. Stieger, B. Hagenbuch, J. Madon, L. Landmann, J. Roth, A. F. Hofmann, and P. J. Meier.** 1998. The sister of P-glycoprotein represents the canalicular bile salt export pump of mammalian liver. J. Biol. Chem. **273:** 10046–10050.
18. **Guler, H. P., J. Zapf, C. Schmid, and E. R. Froesch.** 1989. Insulin-like growth factors I and II in healthy man. Estimations of half-lives and production rates. Acta Endocrinol. **121:**753–758.
19. **Guo, S., G. Rena, S. Cichy, X. He, P. Cohen, and T. Unterman.** 1999. Phosphorylation of serine 256 by protein kinase B disrupts transactivation by FKHR and mediates effects of insulin on insulin-like growth factor-binding protein-1 promoter activity through a conserved insulin response sequence. J. Biol. Chem. **274:**17184–17192.
20. **Hanson, R. W., and L. Reshef.** 1997. Regulation of phosphoenolpyruvate carboxykinase (GTP) gene expression. Annu. Rev. Biochem. **66:**581–611.
21. **Harnish, D. C., S. Malik, E. Kilbourne, R. Costa, and S. K. Karathanasis.** 1996. Control of apolipoprotein AI gene expression through synergistic interactions between hepatocyte nuclear factors 3 and 4. J. Biol. Chem. **271:** 13621–13628.
22. **Herlong, H. F.** 1994. Approach to the patient with abnormal liver enzymes. Hosp. Pract. **29:**32–38.
23. **Hue, L., and G. G. Rousseau.** 1993. Fructose 2,6-bisphosphate and the control of glycolysis by growth factors, tumor promoters and oncogenes. Adv. Enzyme Regul. **33:**97–110.
24. **Kaestner, K. H., H. Hiemisch, and G. Schutz.** 1998. Targeted disruption of

the gene encoding hepatocyte nuclear factor 3γ results in reduced transcription of hepatocyte-specific genes. Mol. Cell. Biol. **18:**4245–4251.
25. **Kaufmann, E., and W. Knochel.** 1996. Five years on the wings of fork head. Mech. Dev. **57:**3–20.
26. **Koopen, N. R., H. Wolters, P. Voshol, B. Stieger, R. J. Vonk, P. J. Meier, F. Kuipers, and B. Hagenbuch.** 1999. Decreased Na^+-dependent taurocholate uptake and low expression of the sinusoidal Na^+-taurocholate cotransporting protein (Ntcp) in livers of mdr2 P-glycoprotein-deficient mice. J. Hepatol. **30:**14–21.
27. **Lai, E., V. R. Prezioso, E. Smith, O. Litvin, R. H. Costa, and J. E. Darnell, Jr.** 1990. HNF-3A, a hepatocyte-enriched transcription factor of novel structure, is regulated transcriptionally. Genes Dev. **4:**1427–1436.
28. **Lai, E., V. R. Prezioso, W. F. Tao, W. S. Chen, and J. E. Darnell, Jr.** 1991. Hepatocyte nuclear factor 3α belongs to a gene family in mammals that is homologous to the *Drosophila* homeotic gene fork head. Genes Dev. **5:** 416–427.
29. **Landry, C., F. Clotman, T. Hioki, H. Oda, J. J. Picard, F. P. Lemaigre, and G. G. Rousseau.** 1997. HNF-6 is expressed in endoderm derivatives and nervous system of the mouse embryo and participates to the cross-regulatory network of liver-enriched transcription factors. Dev. Biol. **192:**247–257.
30. **Lee, Y. H., B. Sauer, P. F. Johnson, and F. J. Gonzalez.** 1997. Disruption of the c/ebpα gene in adult mouse liver. Mol. Cell. Biol. **17:**6014–6022.
31. **Lemaigre, F. P., S. M. Durviaux, and G. G. Rousseau.** 1993. Liver-specific factor binding to the liver promoter of a 6-phosphofructo-2-kinase/fructose-2,6-bisphosphatase gene. J. Biol. Chem. **268:**19896–19905.
32. **Lemaigre, F. P., S. M. Durviaux, O. Truong, V. J. Lannoy, J. J. Hsuan, and G. G. Rousseau.** 1996. Hepatocyte nuclear factor 6, a transcription factor that contains a novel type of homeodomain and a single cut domain. Proc. Natl. Acad. Sci. USA **93:**9460–9464.
33. **Lin, B., D. W. Morris, and J. Y. Chou.** 1997. The role of HNF1α, HNF3γ, and cyclic AMP in glucose-6-phosphatase gene activation. Biochemistry **36:** 14096–14106.
34. **Liu, J. K., C. M. DiPersio, and K. S. Zaret.** 1991. Extracellular signals that regulate liver transcription factors during hepatic differentiation in vitro. Mol. Cell. Biol. **11:**773–784.
35. **Mahl, T. C.** 1998. Approach to the patient with abnormal liver tests. Lippincotts Prim. Care Pract. **2:**379–389.
36. **Makishima, M., A. Y. Okamoto, J. J. Repa, H. Tu, R. M. Learned, A. Luk, M. V. Hull, K. D. Lustig, D. J. Mangelsdorf, and B. Shan.** 1999. Identification of a nuclear receptor for bile acids. Science **284:**1362–1365.
37. **Marsden, I., C. Jin, and X. Liao.** 1998. Structural changes in the region directly adjacent to the DNA-binding helix highlight a possible mechanism to explain the observed changes in the sequence-specific binding of winged helix proteins. J. Mol. Biol. **278:**293–299.
38. **McPherson, C. E., E. Y. Shim, D. S. Friedman, and K. S. Zaret.** 1993. An active tissue-specific enhancer and bound transcription factors existing in a precisely positioned nucleosomal array. Cell **75:**387–398.
39. **Millonig, J. H., J. A. Emerson, J. M. Levorse, and S. M. Tilghman.** 1995. Molecular analysis of the distal enhancer of the mouse α-fetoprotein gene. Mol. Cell. Biol. **15:**3848–3856.
40. **Molowa, D. T., W. S. Chen, G. M. Cimis, and C. P. Tan.** 1992. Transcriptional regulation of the human cholesterol 7α-hydroxylase gene. Biochemistry **31:**2539–2544.
41. **Monaghan, A. P., K. H. Kaestner, E. Grau, and G. Schutz.** 1993. Postimplantation expression patterns indicate a role for the mouse forkhead/HNF-3 α, β and γ genes in determination of the definitive endoderm, chordamesoderm and neuroectoderm. Development **119:**567–578.
42. **Muller, M., and P. L. Jansen.** 1997. Molecular aspects of hepatobiliary transport. Am. J. Physiol. **272:**G1285–G1303.
43. **Nolten, L. A., P. H. Steenbergh, and J. S. Sussenbach.** 1996. The hepatocyte nuclear factor 3β stimulates the transcription of the human insulin-like growth factor I gene in a direct and indirect manner. J. Biol. Chem. **271:** 31846–31854.
44. **Overdier, D. G., A. Porcella, and R. H. Costa.** 1994. The DNA-binding specificity of the hepatocyte nuclear factor 3/forkhead domain is influenced by amino-acid residues adjacent to the recognition helix. Mol. Cell. Biol. **14:** 2755–2766.
45. **Pani, L., X. B. Qian, D. Clevidence, and R. H. Costa.** 1992. The restricted promoter activity of the liver transcription factor hepatocyte nuclear factor 3β involves a cell-specific factor and positive autoactivation. Mol. Cell. Biol. **12:**552–562.
46. **Peterson, R. S., D. E. Clevidence, H. Ye, and R. H. Costa.** 1997. Hepatocyte nuclear factor-3α promoter regulation involves recognition by cell-specific factors, thyroid transcription factor-1 and autoactivation. Cell Growth Differ. **8:**69–82.
47. **Pierreux, C. E., J. Stafford, D. Demonte, D. K. Scott, J. Vandenhaute, R. M. O'Brien, D. K. Granner, G. G. Rousseau, and F. P. Lemaigre.** 1999. Antiglucocorticoid activity of hepatocyte nuclear factor-6. Proc. Natl. Acad. Sci. USA **96:**8961–8966.
48. **Poli, V.** 1998. The role of C/EBP isoforms in the control of inflammatory and native immunity functions. J. Biol. Chem. **273:**29279–29282.
49. **Powell-Braxton, L., P. Hollingshead, C. Warburton, M. Dowd, S. Pitts-Meek, D. Dalton, N. Gillett, and T. A. Stewart.** 1993. IGF-I is required for normal embryonic growth in mice. Genes Dev. **7:**2609–2617.
50. **Qian, X., U. Samadani, A. Porcella, and R. H. Costa.** 1995. Decreased expression of hepatocyte nuclear factor 3α during the acute-phase response influences transthyretin gene transcription. Mol. Cell. Biol. **15:**1364–1376.
51. **Rajkumar, K., D. Barron, M. S. Lewitt, and L. J. Murphy.** 1995. Growth retardation and hyperglycemia in insulin-like growth factor binding protein-1 transgenic mice. Endocrinology **136:**4029–4034.
52. **Rausa, F., U. Samadani, H. Ye, L. Lim, C. F. Fletcher, N. A. Jenkins, N. G. Copeland, and R. H. Costa.** 1997. The cut-homeodomain transcriptional activator HNF-6 is coexpressed with its target gene HNF-3β in the developing murine liver and pancreas. Dev. Biol. **192:**228–246.
53. **Rausa, F. M., L. Galarneau, B. I. L, and R. H. Costa.** 1999. The nuclear receptor fetoprotein transcription factor is coexpressed with its target gene HNF-3β in the developing murine liver intestine and pancreas. Mech. Dev. **89:**185–188.
54. **Raymondjean, M., A. L. Pichard, C. Gregori, F. Ginot, and A. Kahn.** 1991. Interplay of an original combination of factors: C/EBP, NFY, HNF-3 and HNF-1 in the rat aldolase B gene promoter. Nucleic Acids Res. **19:**6145–6153.
55. **Rechler, M. M.** 1993. Insulin-like growth factor binding proteins. Vitam. Horm. **47:**1–114.
56. **Ruiz i Altaba, A., V. R. Prezioso, J. E. Darnell, and T. M. Jessell.** 1993. Sequential expression of HNF-3β and HNF-3α by embryonic organizing centers: the dorsal lip/node, notochord and floor plate. Mech. Dev. **44:** 91–108.
57. **Samadani, U., and R. H. Costa.** 1996. The transcriptional activator hepatocyte nuclear factor six regulates liver gene expression. Mol. Cell. Biol. **16:** 6273–6284.
58. **Samadani, U., X. Qian, and R. H. Costa.** 1996. Identification of a transthyretin enhancer sequence that selectively binds the hepatocyte nuclear factor-3β isoform. Gene Expression **6:**23–33.
59. **Sasaki, H., and B. L. Hogan.** 1993. Differential expression of multiple fork head related genes during gastrulation and axial pattern formation in the mouse embryo. Development **118:**47–59.
60. **Shim, E. Y., C. Woodcock, and K. S. Zaret.** 1998. Nucleosome positioning by the winged helix transcription factor HNF3. Genes Dev. **12:**5–10.
61. **Sjogren, K., J. L. Liu, K. Blad, S. Skrtic, O. Vidal, V. Wallenius, D. LeRoith, J. Tornell, O. G. Isaksson, J. O. Jansson, and C. Ohlsson.** 1999. Liver-derived insulin-like growth factor I (IGF-I) is the principal source of IGF-I in blood but is not required for postnatal body growth in mice. Proc. Natl. Acad. Sci. USA **96:**7088–7092.
62. **Smit, J. J., A. H. Schinkel, R. P. Oude Elferink, A. K. Groen, E. Wagenaar, L. van Deemter, C. A. Mol, R. Ottenhoff, N. M. van der Lugt, M. A. van Roon, M. A. van der Valk, G. J. Offerhaus, A. J. Berns, and P. Borst.** 1993. Homozygous disruption of the murine mdr2 P-glycoprotein gene leads to a complete absence of phospholipid from bile and to liver disease. Cell **75:** 451–462.
63. **Torchia, E. C., S. K. Cheema, and L. B. Agellon.** 1996. Coordinate regulation of bile acid biosynthetic and recovery pathways. Biochem. Biophys. Res. Commun. **225:**128–133.
64. **Trauner, M., P. J. Meier, and J. L. Boyer.** 1998. Molecular pathogenesis of cholestasis. N. Engl. J. Med. **339:**1217–1227.
65. **Tsutsui, T., B. Hesabi, D. S. Moons, P. P. Pandolfi, K. S. Hansel, A. Koff, and H. Kiyokawa.** 1999. Targeted disruption of CDK4 delays cell cycle entry with enhanced p27(Kip1) activity. Mol. Cell. Biol. **19:**7011–7019
66. **Unterman, T. G., A. Fareeduddin, M. A. Harris, R. G. Goswami, A. Porcella, R. H. Costa, and R. G. Lacson.** 1994. Hepatocyte nuclear factor-3 (HNF-3) binds to the insulin response sequence in the IGF binding protein-1 (IGFBP-1) promoter and enhances promoter function. Biochem. Biophys. Res. Commun. **203:**1835–1841.
67. **Unterman, T. G., D. T. Oehler, M. B. Gotway, and P. W. Morris.** 1990. Production of the rat type 1 insulin-like growth factor binding protein (rIGFBP-1) by well-differentiated H4EIIC3 hepatoma cells: identification, purification, and N-terminal amino acid analysis. Endocrinology **127:**789–797.
68. **Vallet, V., B. Antoine, P. Chafey, A. Vandewalle, and A. Kahn.** 1995. Overproduction of a truncated hepatocyte nuclear factor 3 protein inhibits expression of liver-specific genes in hepatoma cells. Mol. Cell. Biol. **15:**5453–5460.
69. **Vos, T. A., G. J. Hooiveld, H. Koning, S. Childs, D. K. Meijer, H. Moshage, P. L. Jansen, and M. Muller.** 1998. Up-regulation of the multidrug resistance genes, Mrp1 and Mdr1b, and down-regulation of the organic anion transporter, Mrp2, and the bile salt transporter, Spgp, in endotoxemic rat liver. Hepatology **28:**1637–1644.
70. **Wang, N. D., M. J. Finegold, A. Bradley, C. N. Ou, S. V. Abdelsayed, M. D. Wilde, L. R. Taylor, D. R. Wilson, and G. J. Darlington.** 1995. Impaired energy homeostasis in C/EBPα knockout mice. Science **269:**1108–1112.
71. **Wang, D. P., D. Stroup, M. Marrapodi, M. Crestani, G. Galli, and J. Y. Chiang.** 1996. Transcriptional regulation of the human cholesterol 7 α-hydroxylase gene (CYP7A) in HepG2 cells. J. Lipid Res. **37:**1831–1841.
72. **Wang, J. C., P. E. Stromstedt, T. Sugiyama, and D. K. Granner.** 1999. The

phosphoenolpyruvate carboxykinase gene glucocorticoid response unit: identification of the functional domains of accessory factors HNF3β (hepatic nuclear factor-3β) and HNF4 and the necessity of proper alignment of their cognate binding sites. Mol. Endocrinol. **13:**604–618.

73. **Weinstein, D. C., A. Ruiz i Altaba, W. S. Chen, P. Hoodless, V. R. Prezioso, T. M. Jessell, and J. Darnell, Jr.** 1994. The winged-helix transcription factor HNF-3β is required for notochord development in the mouse embryo. Cell **78:**575–588.
74. **Wu, H., M. Wade, L. Krall, J. Grisham, Y. Xiong, and T. Van Dyke.** 1996. Targeted in vivo expression of the cyclin-dependent kinase inhibitor p21 halts hepatocyte cell-cycle progression, postnatal liver development and regeneration. Genes Dev. **10:**245–260.
75. **Yakar, S., J. L. Liu, B. Stannard, A. Butler, D. Accili, B. Sauer, and D. LeRoith.** 1999. Normal growth and development in the absence of hepatic insulin-like growth factor I. Proc. Natl. Acad. Sci. USA **96:**7324–7329.
76. **Yan, C., R. H. Costa, J. E. Darnell, Jr., J. D. Chen, and T. A. Van Dyke.** 1990. Distinct positive and negative elements control the limited hepatocyte and choroid plexus expression of transthyretin in transgenic mice. EMBO J. **9:** 869–878.
77. **Ye, H., A. Holterman, K. W. Yoo, R. R. Franks, and R. H. Costa.** 1999. Premature expression of the winged helix transcription factor HFH-11B in regenerating mouse liver accelerates hepatocyte entry into S-phase. Mol. Cell. Biol. **19:**8570–8580.
78. **Zaret, K.** 1999. Developmental competence of the gut endoderm: genetic potentiation by GATA and HNF3/fork head proteins. Dev. Biol. **209:**1–10.
79. **Zhou, L., L. Lim, R. H. Costa, and J. A. Whitsett.** 1996. Thyroid transcription factor-1, hepatocyte nuclear factor-3β, surfactant protein B, C, and Clara cell secretory protein in developing mouse lung. J. Histochem. Cytochem. **44:** 1183–1193.